

Efficient Approximate Degenerate Ordered Statistics Decoding for Quantum Codes via Reliable Subset Reduction

Ching-Feng Kung, Kao-Yueh Kuo, and Ching-Yi Lai

Abstract—Efficient decoding of quantum codes is crucial for achieving high-performance quantum error correction. In this paper, we introduce the concept of approximate degenerate decoding and integrate it with ordered statistics decoding (OSD). Previously, we proposed a reliability metric that leverages both hard and soft decisions from the output of belief propagation (BP), which is particularly useful for identifying highly reliable subsets of variables. Using the approach of reliable subset reduction, we reduce the effective problem size. Additionally, we identify a degeneracy condition that allows high-order OSD to be simplified to order-0 OSD. By integrating these techniques, we present an ADOSD algorithm that significantly improves OSD efficiency in the code capacity noise model. We demonstrate the effectiveness of our BP+ADOSD approach through extensive simulations on a variety of quantum codes, including generalized hypergraph-product codes, topological codes, lift-connected surface codes, and bivariate bicycle codes. The results indicate that the BP+ADOSD decoder outperforms existing methods, achieving higher error thresholds and enhanced performance at low error rates. Additionally, we validate the efficiency of our approach in terms of computational time, demonstrating that ADOSD requires, on average, the same amount of time as two to three BP iterations on surface codes at a depolarizing error rate of around 1%. All the proposed algorithms are compared using single-threaded CPU implementations.

I. INTRODUCTION

Reliable quantum communication is a critical area of research, essential for scaling quantum systems, enabling the exchange of quantum information across distances, and facilitating multiparty protocols. Quantum states are inherently fragile, requiring the implementation of quantum error correction to mitigate the effects of noise and decoherence [2], [3]. In this work, we explore advanced decoding techniques for quantum error-correcting codes to enhance the reliability and efficiency of quantum communication.

Quantum stabilizer codes, analogous to classical linear block codes, allow efficient encoding and binary syndrome decoding [4]–[6]. A notable class of stabilizer codes is quantum low-density parity-check (LDPC) codes, which are preferred for their high code rates and feasible syndrome measurements from low-weight stabilizers. These codes can be decoded using

belief propagation (BP), similar to classical LDPC codes [7]–[19]. A quantum LDPC code of the Calderbank–Shor–Steane (CSS) type [20], [21] can be decoded by the BP algorithm for binary codes (BP₂) by treating X and Z errors separately. When X and Z errors exhibit correlations, such as in depolarizing channels, a quaternary BP algorithm (BP₄) could be more effective, as it better exploits the error correlations during decoding. An important feature of quantum codes is their binary error syndromes, unlike classical nonbinary codes. Consequently, the complexity of BP₄ can be reduced by restricting message passing in the Tanner graph [12] to scalar messages, which encode the likelihood ratios associated with Pauli commutation relations.

The decoding problem for quantum codes with high degeneracy is particularly challenging for BP, as seen in topological codes [22]–[28]. To address these challenges, several remedies for the BP algorithm have been introduced, including techniques such as random perturbation [8], enhanced feedback [9], [10], check-matrix augmentation [11], message normalization and offset [12], [13], and trapping set analysis [29], [30]. These methods aim to improve the decoding accuracy and convergence of the BP algorithm. A recently developed modified BP₄ algorithm, known as MBP₄, incorporates additional memory effects and has demonstrated the ability to handle topological codes [31]. The adaptive version of MBP₄, termed AMBP₄, further improves BP performance while maintaining nearly linear time complexity [31]. Nonetheless, its practical application involves an unknown parameter search and may not be fully parallelized.

We investigate ordered statistic decoding (OSD) in quantum coding theory as a complementary approach to BP. Fossorier and Lin [32] first proposed OSD in classical coding theory as an approach to approximate maximum-likelihood decoding [33]–[41]. The OSD algorithm searches for possible solutions by sorting the reliability measures of symbols while maintaining controllable complexity [32], [42]–[45]. In cases where BP fails to find a valid error for a given syndrome, syndrome-based OSD can be utilized [46]. Moreover, OSD has been demonstrated to be particularly useful for degenerate quantum codes by Pantelev and Kalachev [42].

The core function of OSD is Gaussian elimination on the parity-check matrix of dimension $m \times n$, which identifies the independent unreliable bits and has a complexity of $\mathcal{O}(nm^2)$. The remaining reliable bits can be used to regenerate the most probable error. In an order- w OSD, the set of reliable bits can be flipped up to w bits, generating a list of probable solutions.

This article was presented in part at the 2023 International Symposium on Topics in Coding (ISTC) [1].

CFK and CYL are with the Institute of Communications Engineering, National Yang Ming Chiao Tung University (NYCU), Hsinchu 300093, Taiwan. (email: cylai@nycu.edu.tw)

KYK is with the School of Mathematical and Physical Sciences, University of Sheffield, UK.

However, this technique incurs at least a cubic time complexity overhead from Gaussian elimination, along with additional costs for high-order examination, despite its effectiveness.

Fossorier *et al.* [46] identified specific candidate pruning conditions to reduce ineffective high-order OSD processing, as such operations do not yield improved error candidates. Many techniques have been proposed in classical coding theory to reduce the complexity of high-order OSD, by focusing on more probable candidates, thereby reducing the number of OSD candidates required [47]–[52].

Similarly, in the quantum regime, the OSD schemes in [42], [43] focus on bit-flips of less reliable bits, but the overhead of order-0 OSD (OSD-0) remains dominant. Roffe *et al.* [43] proposed a BP2-OSD-CS λ decoder with a greedy search for a combination sweep, typically set to $\lambda = 60$. iOlius and Martinez [53] introduced a closed-branch (CB) decoder as a lower-complexity alternative to OSD, though BP+CB underperforms compared to BP-OSD-0. Gong *et al.* [54] introduced the guided decimation guessing (GDG) decoder, achieving performance comparable to BP2-OSD-CS10 and surpassing BP-OSD-0 for bivariate bicycle (BB) codes [55]. To reduce the computational overhead in Gaussian elimination, Wolanski and Barber proposed the ambiguity clustering decoder [56], and Hillmann *et al.* proposed localized statistics decoding (LSD) [57]. Both are divide-and-conquer algorithms, as they partition the decoding problem into smaller subproblems based on specific heuristics.

However, there is a great deal of room for improvement over the current postprocessing techniques in the literature under the code capacity noise model. These methods primarily rely on binary BP to handle quaternary errors, neglecting error correlations, which suggests that binary decoders are inherently suboptimal. In contrast, the quaternary AMBP $_4$ decoder in [31] has been shown to outperform all the aforementioned decoders without requiring postprocessing. For supporting examples, please refer to Figure 2, Figure 4, and Figure 7 in the simulation section.

Since OSD acts as a complementary strategy to BP for cases where BP fails, BP-OSD is naturally expected to surpass the performance of AMBP $_4$. In this paper, we propose a BP $_4$ -based OSD to achieve this improvement. Additionally, we introduce an efficient OSD algorithm tailored for quantum codes.

First, the sorting process plays a pivotal role in OSD [32]. For efficient implementation, we consider binary representations of an n -qubit quantum code and thus an n -qubit Pauli error variable can be represented by $2n$ binary variables. Previously we proposed a reliability metric that takes into account the hard-decision history obtained during BP $_4$ iterations and incorporates soft messages from the last iteration [1]. The $2n$ binary error variables of an error vector are then sorted according to the reliability metric. Specifically, the length of the last run in a bit’s hard-decision history is the primary term in our metric. Through simulations, we demonstrate that incorporating the hard-decision history to determine the reliability order for OSD enhances decoding performance. Our OSD algorithm based on this reliability metric will be denoted as OSD $_4$.

To develop an efficient OSD algorithm, it is crucial to reduce the problem size in OSD and minimize the computational burden of Gaussian elimination. To address this challenge, we propose an approach called *reliable subset reduction*. In the code capacity error decoding problem of an $[[n, k]]$ quantum code, we need to solve a linear system of equations with $2n$ binary variables and $n - k$ independent constraints. The core idea is that if the solution for a subset of the variables can be determined with confidence, the linear system can be reduced, thereby lowering the computation burden of both Gaussian elimination and the OSD process. So the primary task is to identify a highly reliable subset. An excellent choice are the bits that exhibit nearly constant hard decision history vectors during BP $_4$ iterations and show high soft reliability in the final iteration. At low error rates, there is a large portion of highly reliable bits. Eliminating these bits would significantly accelerate the OSD process. Moreover, resources can be allocated to the less reliable parts, similar to the approaches in [42], [43]. We will demonstrate that in our simulations of surface codes with distances from 11 to 15, the problem sizes are reduced to less than 30% of the original in over 90% of the trials at an error rate of around 2%. We note that the ambiguity clustering decoder [56] and LSD [57] operate at a different stage from our approach, and these algorithms could be applied after reliable subset reduction.

Next, we consider approximate degenerate OSD in quantum codes. A typical OSD generates a list of error candidates for a given error syndrome and selects the one with the minimum weight, which is optimal for classical codes. For quantum codes, however, the optimal decoding criterion involves choosing the error coset with the highest probability, a criterion that is challenging to implement in practice. To address this, we consider approximate degenerate decoding in OSD by focusing only on relatively low-weight terms within an error coset.

Additionally, we introduce a degenerate error candidate pruning condition for stabilizer codes. We show that certain bit-flips in OSD correspond to multiplying stabilizers, resulting to degenerate error candidates. These bit-flips may alter the error weight but do not change the error coset, allowing them to be ignored in approximate degenerate OSD. For improving OSD efficiency, using a minimum weight decoding criterion is beneficial. A key observation is that if all bit-flips correspond to multiplying a stabilizer, there is no need to implement high-order OSD. We will demonstrate that this is indeed the case at low error rates by simulations in Section VI-G. We note that a degeneracy condition is also utilized in ambiguity clustering to facilitate the resolution of subproblems [56].

Integrating all the mentioned techniques, we propose an approximate degenerate OSD algorithm, abbreviated as ADOSD $_4$. We conduct simulations of MBP $_4$ and our OSD schemes OSD $_4$ and ADOSD $_4$ on several quantum codes under depolarizing errors in the code capacity noise model, including BB codes [55], rotated toric codes and rotated surface codes [24], (6.6.6) and (4.8.8) color codes [27], twisted XZZX codes on a torus [58], generalized hypergraph-product (GHP) codes [42], [43], and lift-connected surface (LCS) codes [59].

The results demonstrate that our proposed schemes out-

perform previous approaches in the literature, both in terms of error thresholds for topological codes and low error rate performance (logical error rate around 10^{-6}). Both our $\text{MBP}_4+\text{OSD}_4$ and $\text{MBP}_4+\text{ADOSD}_4$ decoders outperform other binary BP-OSD schemes in these quantum codes. We achieve thresholds of approximately 17.5%–17.7% for the toric, surface, and twisted XZZX codes, and thresholds of 15%–15.42% for the (4.8.8) and (6.6.6) color codes, as summarized in Table II. Comparisons of our results with existing threshold values for the toric codes are provided in Table III. We also compare the performance of various reliability metrics on the GHP code, justifying our choice of reliability metric.

Finally, we analyze the time efficiency of our OSD schemes for various topological codes of comparable distances to the $[[882, 48, 16]]$ GHP code using single-threaded CPU implementations. The simulation results, summarized in Table IV, show that the time consumption of ADOSD_4 is approximately 1% to 3% of that for order-2 OSD_4 with similar decoding performance. Moreover, Table VI presents the time consumption of ADOSD_4 in terms of BP iterations for surface codes with distances from 11 to 15. Specifically, the average time consumption per codeword for ADOSD_4 is approximately equivalent to 2 to 3 BP_4 iterations, whereas a successful BP trial typically takes 2 to 3 iterations on average. This suggests that ADOSD_4 is an excellent complement to BP, especially since ADOSD_4 is used only when BP fails.

This paper is organized as follows. We introduce quantum stabilizer codes in Section II. Section III discusses reliability metrics and the associated OSD algorithm. The reliable subset reduction method is presented in Section IV. We then cover approximate degenerate decoding in Section V, and provide simulation results in Section VI. Finally, we conclude in Sec. VII.

II. QUANTUM STABILIZER CODES

In this section, we review the basic of stabilizer codes and define the relevant notation [4]–[6].

Let $I = \begin{bmatrix} 1 & 0 \\ 0 & 1 \end{bmatrix}$, $X = \begin{bmatrix} 0 & 1 \\ 1 & 0 \end{bmatrix}$, $Z = \begin{bmatrix} 1 & 0 \\ 0 & -1 \end{bmatrix}$, and $Y = iXZ$ denote the Pauli matrices. Consider the n -fold Pauli group

$$\mathcal{G}_n \triangleq \{cM_1 \otimes \cdots \otimes M_n : c \in \{\pm 1, \pm i\}, M_j \in \{I, X, Y, Z\}\}.$$

Every nonidentity Pauli operator in \mathcal{G}_n has eigenvalues ± 1 . Any two Pauli operators either commute or anticommute with each other. The weight of a Pauli operator $E \in \mathcal{G}_n$, denoted $\text{wt}(E)$, refers to the number of its nonidentity components.

We consider Pauli errors in this paper, assuming independent depolarizing errors with rate ϵ . Each qubit independently experiences an X , Y , or Z error with probability $\epsilon/3$ and no error with probability $1 - \epsilon$. Therefore, at a small error rate ϵ , low-weight Pauli errors are more likely to occur.

A *stabilizer group* \mathcal{S} is an Abelian subgroup in \mathcal{G}_n such that $-I^{\otimes n} \notin \mathcal{S}$ [6]. Suppose that \mathcal{S} is generated by $n - k$ independent generators. Then \mathcal{S} defines an $[[n, k, d]]$ stabilizer code $\mathcal{C}(\mathcal{S})$ that encodes k logical qubits into n physical qubits:

$$\mathcal{C}(\mathcal{S}) = \left\{ |\psi\rangle \in \mathbb{C}^{2^n} : S|\psi\rangle = |\psi\rangle, \forall S \in \mathcal{S} \right\}.$$

The elements in \mathcal{S} are called *stabilizers*. The parameter d represents the minimum distance of the code such that any Pauli error of weight less than d is *detectable*.

An error $E \in \mathcal{G}_n$ can be detected by $\mathcal{C}(\mathcal{S})$ through stabilizer measurements if E anticommutes with some of its stabilizers. Suppose that $\{S_i\}_{i=1}^m$, where $m \geq n - k$, is a set of stabilizers that generates \mathcal{S} . Their binary measurement outcomes are referred to as the *error syndrome* of E . Let $N(\mathcal{S}) \subset \mathcal{G}_n$ denote the normalizer group of \mathcal{S} , which consists of the Pauli operators that commute with all stabilizers. Consequently, if an error is in $N(\mathcal{S})$, it will have zero syndrome and cannot be detected. Note that if an error is a stabilizer, it has no effect on the code space. An element in the normalizer group $N(\mathcal{S})$ that is not a stabilizer, up to a phase, is called a *nontrivial logical operator as it changes the logical state of a code*. Therefore, the minimum distance of $\mathcal{C}(\mathcal{S})$ is defined as the minimum weight of a nontrivial logical operator. It can be observed that E and ES for $S \in \mathcal{S}$ have the same effects on the codespace. They are called *degenerate* to each other. We say that a quantum code is *highly degenerate* if it has many stabilizers with low weight relative to its minimum distance.

A syndrome decoding problem can be stated as follows: given an error syndrome of an unknown Pauli error E , find the most probable $\hat{E} \in \mathcal{G}_n$ that matches the syndrome. An error estimate \hat{E} is considered *valid* if it matches the syndrome or $\hat{E}E \in \mathcal{S}$. Two decoding criteria are typically considered: minimum weight decoding and degenerate maximum likelihood decoding [60]–[62]. In minimum weight decoding, the error \hat{E} with the smallest weight is chosen, while in degenerate maximum likelihood decoding, the error \hat{E} whose coset $\hat{E}\mathcal{S}$ has the minimum coset probability is selected. However, degenerate maximum likelihood decoding has exponential complexity and is impractical due to the need for coset enumeration. We propose the following criterion.

Definition 1. (Approximate Degenerate Decoding)

A δ -approximate degenerate decoding (δ -ADD) criterion aims to find an error estimate \hat{E} that matches the given syndrome, maximizing the dominant terms of its coset probability

$$\sum_{S \in \mathcal{S}, \text{wt}(S) \leq \delta} \Pr \{ \hat{E}S \}. \quad (1)$$

Note that 0-ADD reduces to minimum weight decoding, while n -ADD corresponds precisely to degenerate maximum likelihood decoding.

A. Binary representations

Without loss of generality, we assume that each stabilizer in $\{S_i\}_{i=1}^m$ is of the form $S_i = S_{i1} \otimes S_{i2} \otimes \cdots \otimes S_{in}$, where $S_{ij} \in \{I, X, Y, Z\}$. Then we can study the decoding problem in the binary vector space [4], [6], using a mapping φ :

$$I \mapsto [0 \mid 0], X \mapsto [1 \mid 0], Z \mapsto [0 \mid 1], Y \mapsto [1 \mid 1].$$

A *check matrix* of the stabilizer code $\mathcal{C}(\mathcal{S})$ is a binary matrix $\mathbf{S} = [\mathbf{S}_{ij}] \in \{0, 1\}^{m \times 2n}$, where

$$[\mathbf{S}_{ij} \mid \mathbf{S}_{i(j+n)}] = \varphi(S_{ij}).$$

An n -fold Pauli operator $E \in \mathcal{G}_n$ can also be represented by $\varphi(E) \triangleq \mathbf{E} = \begin{bmatrix} \mathbf{E}^X & | & \mathbf{E}^Z \end{bmatrix} \in \{0, 1\}^{2n}$, where \mathbf{E}^X and \mathbf{E}^Z are the indicator vectors of X and Z components of E , respectively. Then the error syndrome of E is

$$\mathbf{z} = \mathbf{S}\mathbf{A}\mathbf{E}^\top \in \{0, 1\}^{m \times 1}, \quad (2)$$

where \mathbf{E}^\top denotes the transpose of \mathbf{E} , $\mathbf{A} = \begin{bmatrix} \mathbf{0} & | & \mathbf{I}_n \\ \mathbf{I}_n & | & \mathbf{0} \end{bmatrix}$, \mathbf{I}_n is the $n \times n$ identity matrix, and $\mathbf{0}$ is the zero matrix of appropriate dimensions.

Consequently, the decoding problem is to solve this system of linear equations with $2n$ binary variables \mathbf{E}_j that are most probable. Note that \mathbf{S} is of rank $n-k$ so the degree of freedom of this binary system is $n+k$.

B. Belief Propagation (BP) Decoding

We explain how a quaternary BP algorithm works in the following [12], which is computed in linear domain. A log-likelihood version of BP can be found in [13].

Given a check matrix \mathbf{S} , a syndrome \mathbf{z} , and a depolarizing error rate ϵ , BP performs the following steps:

- 1) An initial error distribution $\mathbf{p}_i \in \mathbb{R}^4$ for qubit $i \in \{1, 2, \dots, n\}$ is chosen for BP.
- 2) The belief distribution vector $\mathbf{q}_i = (q_i^I, q_i^X, q_i^Y, q_i^Z)$ will be updated by BP, using the messages of parity-check satisfaction and the channel statistics \mathbf{p}_i for $i = 1, 2, \dots, n$.
- 3) At each iteration, an error estimate $\hat{\mathbf{E}} \in \{0, 1\}^{2n}$ is made according to the hard decision on \mathbf{q}_i . If a valid error estimate is generated, it will be accepted as the solution; otherwise, go to the next iteration starting from step 2).

Steps 2) and 3) will be iterated for a maximum number of T iterations, where T is chosen in advance. If no valid estimate is obtained after T iterations, BP will claim a failure.

Typically, the initial error distribution \mathbf{p}_i is defined as $(1 - \epsilon, \frac{\epsilon}{3}, \frac{\epsilon}{3}, \frac{\epsilon}{3})$. However, one may instead choose a fixed initialization by a given value $\epsilon_0 \neq \epsilon$ for BP as long as BP performs well at this ϵ_0 . See more discussion on fixed initialization in [13], [31], [63].

III. ORDER-STATISTIC DECODING BASED ON QUATERNARY BELIEF PROPAGATION

In the aforementioned syndrome decoding problem, we aim to solve a system of linear equations given by (2), for a given parity-check matrix \mathbf{S} and an error syndrome \mathbf{z} with $2n$ binary variables. The linear system has $n-k$ independent constraints, implying that there are $n+k$ degrees of freedom in the vector \mathbf{E} . Given the values of these $n+k$ bits, one can reconstruct \mathbf{E} . If BP fails to provide a valid error estimate after T iterations, OSD will be utilized.

In the context of OSD, a critical step involves identifying and sorting the accurate and reliable coordinates to establish $n+k$ linearly independent bits. Then, we can use these coordinates to generate a valid error that matches the syndrome. To accomplish this, it is necessary to establish the concept of reliability order as a means of prioritizing the coordinates based on their reliability.

A. Reliability order based on BP₄

To utilize the quaternary distribution generated by BP₄ for each qubit error in OSD, we propose a method that employs the hard-decision history from all BP iterations and the output probabilities from the last BP iteration.

Suppose that BP fails to provide a valid error after a maximum of T iterations. At this point, we have the output distribution $\mathbf{q}_i = (q_i^I, q_i^X, q_i^Y, q_i^Z)$, $i = 1, 2, \dots, n$ from the last BP iteration. Additionally, we have the hard-decision results for all T iterations, denoted by $\mathbf{h}_i^{(j)} \in \{I, X, Y, Z\}$ for $i = 1, \dots, n$ and $j = 1, \dots, T$. For example, $\mathbf{h}_i^{(1)}, \mathbf{h}_i^{(2)}, \dots, \mathbf{h}_i^{(T)}$ represent the hard-decision result history of BP at qubit i and $\mathbf{h}_1^{(j)}, \mathbf{h}_2^{(j)}, \dots, \mathbf{h}_n^{(j)}$ represent the hard-decision results of BP at the j -th iteration.

Our objective is to assign reliability for each Pauli X and Z error. Following the reliability definitions in our previous paper [1], we define two types of measures in the following.

Definition 2. Define a *hard-decision reliability vector* $\boldsymbol{\eta} = (\eta_1, \dots, \eta_n) \in \mathbb{Z}^n$ such that η_i represents the number of consecutive iterations during which the error at qubit i remains unchanged until the final hard decision is made.

In other words, η_i is the length of the last run in the string $\mathbf{h}_i^{(1)}, \mathbf{h}_i^{(2)}, \dots, \mathbf{h}_i^{(T)}$. For example, if the hard-decision outputs at the first qubit over the last five iterations are X, Y, Z, Z, Z , then the final hard decision output is Z and $\eta_1 = 3$. This means that the error at qubit 1 persisted unchanged as Z for three iterations when BP stops.

For implementation, storing the entire hard-decision history \mathbf{h} is unnecessary. One can record only the hard-decision outputs at the latest iteration and uses the latest belief vector \mathbf{q}_i to update the values of $\{\eta_i : i = 1, \dots, n\}$.

Our modified BP₄ algorithm, which incorporates hard-decision reliability measures, is presented in Algorithm 1.

When BP fails, we are left with belief distributions $\mathbf{q}_i = (q_i^I, q_i^X, q_i^Y, q_i^Z)$ for $i = 1, 2, \dots, n$, which will be utilized in the reliability measure.

Definition 3. Define two *soft reliability functions*

$$\begin{aligned} \phi^X(i) &= \max\{q_i^X + q_i^Y, q_i^I + q_i^Z\}, \\ \phi^Z(i) &= \max\{q_i^Z + q_i^Y, q_i^I + q_i^X\}, \end{aligned}$$

for $i \in \{1, 2, \dots, n\}$.

Note that $\{q_i^X + q_i^Y, q_i^I + q_i^Z\}$ is a binary distribution indicating the likelihood of an X error occurring at the i -th qubit and similarly for $\{q_i^X + q_i^Y, q_i^I + q_i^Z\}$.

Now we define a reliability order for the bits in $\mathbf{E} = \begin{bmatrix} \mathbf{E}^X & | & \mathbf{E}^Z \end{bmatrix} \in \{0, 1\}^{2n}$ based on the outputs of BP₄, using the aforementioned hard and soft reliability functions.

Definition 4. For $1 \leq i, j \leq n$ and $a, b \in \{X, Z\}$, error bit \mathbf{E}_i^a is said to be *more reliable* than error bit \mathbf{E}_j^b if $\eta_i > \eta_j$, or if $\phi^a(i) \geq \phi^b(j)$ when $\eta_i = \eta_j$.

This definition means that the hard-decision history reliability is used to rank the error coordinates, with the soft reliability serving as a tie-breaker.

Algorithm 1 BP₄

Input: check matrix $\mathbf{S} \in \{0, 1\}^{m \times 2n}$, syndrome $\mathbf{z} \in \{0, 1\}^{m \times 1}$, depolarizing error rate ϵ , maximum number of iterations T .

Output: A valid error estimate $\hat{\mathbf{E}} \in \{0, 1\}^{2n}$ and belief distributions $\{\mathbf{q}_i\}_{i=1}^n$.

Initialization:

Choose initial error distributions $\mathbf{p}_i \in \mathbb{R}^4$ for $i = 1, \dots, n$.

Let $\eta_i = 1$ for $i = 1, \dots, n$. Let $\mathbf{h}_i = I$ for $i = 1, \dots, n$.

Let $\mathbf{q}_i = \mathbf{0}$ for $i = 1, \dots, n$.

Steps:

for $j = 1$ to T **do**

Update $\{\mathbf{q}_i\}_{i=1}^n$, using \mathbf{S} , \mathbf{z} , and $\{\mathbf{p}_i\}_{i=1}^n$.

for $i = 1$ to n **do**

if $\mathbf{h}_i = \text{HardDecision}(\mathbf{q}_i)$ **then** $\eta_i \leftarrow \eta_i + 1$;

else $\mathbf{h}_i \leftarrow \text{HardDecision}(\mathbf{q}_i)$. $\eta_i = 1$.

end if

end for

if the hard-decision \mathbf{h} matches the syndrome \mathbf{z} **then**

return $\varphi(\mathbf{h})$ and $\{\mathbf{q}_i\}_{i=1}^n$.

end if

end for

return $\mathbf{0}$ and $\{\mathbf{q}_i\}_{i=1}^n$. ▷ BP fails.

Let \mathbf{E} be the hard-decision output from BP₄ after T iterations. If \mathbf{E} does not match the syndrome, OSD will be applied. We now present our OSD algorithm based on the reliability orders as in Algorithm 2, which is also referred to as OSD₄₋₀. If the bits in the reliable subset are correct, the output of OSD₄₋₀ is the required solution.

For comparison with conventional OSD procedures that do not incorporate the history of BP hard-decision outputs across iterations, we also define a reliability order that accounts for only the soft reliability functions of BP₄.

Definition 5. Error bit \mathbf{E}_i^a is said to be *more reliable* than error bit \mathbf{E}_j^b in the marginal distribution if $\phi^a(i) \geq \phi^b(j)$.

An OSD algorithm that follows a reliability order depending only on the belief distributions from the last BP iteration is referred to as mOSD. The OSD based on Definition 5 is referred to as mOSD₄.

Note that the reliability metric in Definition 5 is distinct from those in [42], [43]. Other alternative metrics can also be considered, such as

$$\text{(Entropy)} \quad H_4(\mathbf{q}_i) = - \sum_{M \in \{I, X, Y, Z\}} q_i^M \log(q_i^M), \quad (5)$$

$$\text{(Max)} \quad \max(\mathbf{q}_i) = \max_{M \in \{I, X, Y, Z\}} q_i^M. \quad (6)$$

The reliability of qubit i is assessed based on the quaternary entropy of its belief distribution \mathbf{q}_i (Entropy) or based on the maximum probability of the distribution (Max). For our purpose, the hard-decision output of BP is first sorted in the Pauli basis based on the reliability metric (either Entropy or Max) and then transformed into a binary vector for OSD [42]. We will compare these reliability metrics in Section VI-D.

Algorithm 2 OSD₄₋₀

Input: check matrix $\mathbf{S} \in \{0, 1\}^{m \times 2n}$ of rank $n - k$, syndrome $\mathbf{z} \in \{0, 1\}^{m \times 1}$, hard-decision reliability vector $\boldsymbol{\eta} \in \mathbb{Z}^n$, hard-decision vector $\mathbf{E} \in \{0, 1\}^{2n}$, and belief distributions $\{\mathbf{q}_i\}_{i=1}^n$.

Output: A valid error estimate $\hat{\mathbf{E}} \in \{0, 1\}^{2n}$.

Steps:

1: Sort the error bits in ascending order of reliability. Construct a column permutation function π corresponding to the sorting order. Calculate $\pi(\mathbf{E})$ and $\pi(\mathbf{S}\boldsymbol{\Lambda})$.

2: Perform Gaussian elimination on $\pi(\mathbf{S}\boldsymbol{\Lambda})$ and let the output be denoted by $R(\pi(\mathbf{S}\boldsymbol{\Lambda}))$, where R is the corresponding row operations in the Gaussian elimination. If necessary, apply a column permutation function μ to ensure that the first $n - k$ columns of the resulting matrix are linearly independent. Thus we have

$$\mu(R(\pi(\mathbf{S}\boldsymbol{\Lambda}))) = \begin{bmatrix} \mathbf{I}_{n-k} & \mathbf{A} \\ \mathbf{0} & \mathbf{0} \end{bmatrix}, \quad (3)$$

for some $\mathbf{A} \in \{0, 1\}^{(n-k) \times (n+k)}$, where the last $m - (n - k)$ rows are all zeros.

3: Let $\mathbf{z}' = R(\mathbf{z})$ so that the parity-check condition (2) becomes $\mathbf{z}' = \mu(R(\pi(\mathbf{S}\boldsymbol{\Lambda}))) (\mu(\pi(\hat{\mathbf{E}})))^\top$. Remove the last $m - (n - k)$ entries of \mathbf{z}' .

4: Suppose $\mu(\pi(\mathbf{E})) = [\mathbf{E}^U \quad \mathbf{E}^R]$, where \mathbf{E}^U represents the independent and unreliable subset of $n - k$ bits and \mathbf{E}^R is the reliable subset of $n + k$ bits. **return**

$$\hat{\mathbf{E}} \triangleq \pi^{-1} \left(\mu^{-1} \left(\left[\mathbf{z}'^\top \oplus \mathbf{E}^R \mathbf{A}^\top \quad \mathbf{E}^R \right] \right) \right). \quad (4)$$

B. OSD_{4-w}

If some bits in the reliable subset are incorrect, additional processing is necessary. We may flip up to w bits in the reliable subset and generate the corresponding error estimate. If this error estimate is valid, it is an error candidate. This process is repeated for all $\sum_{i=0}^w \binom{n+k}{i}$ possibilities, and the output will be a valid error candidate that is optimal with respect to δ -ADD for a certain δ . This type of OSD algorithm is referred to as order- w OSD₄ (or OSD_{4-w} for short).

In order to explore all $\sum_{i=0}^w \binom{n+k}{i}$ possibilities, we propose to use the depth-first search (DFS) algorithm. Figure 1 illustrates the idea of using DFS to traverse all bit strings of length 4 and with weight at most 2. One can see that a child node is obtained by flipping one zero bit from its parent node. Consequently, one can recursively generate all $\sum_{i=0}^w \binom{n+k}{i}$ possibilities by bit flipping and encoding.

Lemma 6. Given an OSD₄₋₀ output vector, flipping one of its reliable bits to generate an error candidate takes time $\mathcal{O}(n)$. Similarly, generating an error candidate corresponding to a child node from its parent node also takes $\mathcal{O}(n)$ time.

Proof. Consider the vector $[\mathbf{z}'^\top \oplus \mathbf{E}^R \mathbf{A}^\top \mid \mathbf{E}_1^R \mathbf{E}_2^R \cdots \mathbf{E}_{n+k}^R]$ generated by OSD₄₋₀ in (4), where \mathbf{E}_j^R are reliable bits. Suppose that the matrix \mathbf{A} in (3) has columns $\mathbf{A}_1, \mathbf{A}_2, \dots, \mathbf{A}_{n+k} \in \{0, 1\}^{n-k}$. Then flipping the bit \mathbf{E}_i^R

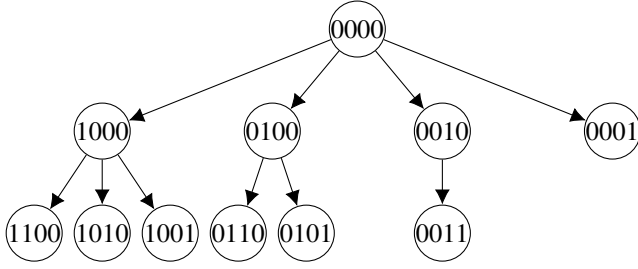


Fig. 1. A tree with nodes consisting of all bit strings of length 4 and with at most weight 2. The root node is 0000. A child node is obtained by flipping one of the zero bits from its parent node that come after the last bit that is one.

generates the vector

$$\left[\mathbf{z}'^\top \oplus \mathbf{E}^R \mathbf{A}^\top \oplus \mathbf{A}_i^\top \mid \mathbf{E}_1^R \mathbf{E}_2^R \cdots (1 \oplus \mathbf{E}_i^R) \cdots \mathbf{E}_{n+k}^R \right], \quad (7)$$

which is a valid error candidate after permutations. It can be checked that this calculation takes time $\mathcal{O}(n)$. \square

To efficiently navigate through these possibilities, we can utilize the technique described in Lemma 6 combining with the DFS algorithm. Then all $\sum_{i=0}^w \binom{n+k}{i}$ candidates can be recursively generated.

We prioritize flipping the least reliable bits first. If an error with a lower Hamming weight is encountered, we update the solution accordingly. However, if the error has the same Hamming weight as the current one, we retain the previous solution since the bit flipped in the previous step is deemed less reliable.

C. Complexity of OSD_4

We analyze the complexity of OSD based on 0-ADD in the following. The complexity of OSD_{4-0} is dominated by the Gaussian elimination step, which is then $\mathcal{O}(2n \times m^2) = \mathcal{O}(n^3)$, assuming $m = \mathcal{O}(n)$. For OSD_{4-w} with $w > 0$, the total number of possible flips is $\sum_{j=0}^w \binom{n+k}{j}$, which can be expressed as $\mathcal{O}((n+k)^w)$ or simply $\mathcal{O}(n^w)$.

In Lemma 6, when we flip a bit in the reliable part, it requires only $\mathcal{O}(n)$ calculations to find an error candidate. Additionally, by running through $\sum_{j=0}^w \binom{n+k}{j}$ possibilities using the DFS algorithm, the OSD_{4-w} algorithm has a complexity of $\mathcal{O}(n^3 + n^{w+1})$, which simplifies to $\mathcal{O}(n^3)$ when $w \leq 2$.

The above OSD complexity is only required when BP fails to converge. BP has a worst-case time complexity of $\mathcal{O}(n\gamma T)$ using a sequential schedule, where n is the number of error variables, γ is the mean column weight of the check matrix, and T is the maximum number of iterations. However, BP typically converges quickly, within $\mathcal{O}(\log N)$ iterations, for sparse matrices. This is also the case for MBP_4 as demonstrated in Table VI in the simulation section. Thus MBP_4 has a nearly linear complexity in n from simulations and has a high probability of convergence for many sparse-graph quantum codes [12], [13].

IV. EFFICIENT OSD WITH HIGHLY RELIABLE SUBSET REDUCTION

As we increase the order w of OSD, we can expect an improvement in the decoder's performance. In particular, when

Algorithm 3 HRSR

Input: check matrix $\mathbf{S} \in \{0, 1\}^{m \times 2n}$ of rank $n - k$, syndrome $\mathbf{z} \in \{0, 1\}^{m \times 1}$, hard-decision reliability vector $\boldsymbol{\eta} \in \mathbb{Z}^n$, hard-decision vector $\mathbf{E} \in \{0, 1\}^{2n}$, belief distributions $\{\mathbf{q}_i\}_{i=1}^n$, and soft reliability threshold θ .

Output: shortened variables $\tilde{\mathbf{z}}, \tilde{\mathbf{S}}, \mathbf{E}^H$, and σ .

Steps:

- 1: Use $\boldsymbol{\eta}$, $\mathbf{q}_{i=1}^n$, and θ to identify the highly reliable bits in \mathbf{E} based on Definition 7. Assume that there are v such highly reliable bits.
- 2: Let σ be a column permutation such that $\sigma(\mathbf{E}) = [\mathbf{E}' \ \mathbf{E}^H]$, where \mathbf{E}^H is the highly reliable subset of v bits, and \mathbf{E}' is the remaining $2n - v$ bits. Let $\sigma(\hat{\mathbf{E}}) = [\hat{\mathbf{E}}' \ \mathbf{E}^H]$ be a permuted error estimate, which contains the highly reliable bits in \mathbf{E}^H .
- 3: Let τ be a row permutation such that $\tau(\sigma(\mathbf{S}\boldsymbol{\Lambda})) = \begin{bmatrix} \tilde{\mathbf{S}} & \mathbf{B} \\ \mathbf{0} & \mathbf{C} \end{bmatrix}$ for $\tilde{\mathbf{S}} \in \{0, 1\}^{m' \times (2n-v)}$ with $m' \leq m$. The $m - m'$ rows $[\mathbf{0} \ \mathbf{C}]$ correspond to parity checks related only to the highly reliable bits. Assume that $\tau(\mathbf{z}) = \begin{bmatrix} \mathbf{z}'' \\ \mathbf{z}^H \end{bmatrix}$, where $\mathbf{z}'' \in \{0, 1\}^{m' \times 1}$, and $\mathbf{z}^H \in \{0, 1\}^{(m-m') \times 1}$ are the syndrome bits corresponding to $[\mathbf{0} \ \mathbf{C}]$.
- 4: Verify the parity check condition related to the highly reliable bits.

if $\mathbf{z}^H \neq \mathbf{C}(\hat{\mathbf{E}}^H)^\top$ **then return failure;**
else we have a new parity-check condition

$$\tilde{\mathbf{z}} = \tilde{\mathbf{S}}(\hat{\mathbf{E}}^H)^\top, \quad (8)$$

where $\tilde{\mathbf{z}} = \mathbf{z}'' - \mathbf{B}(\hat{\mathbf{E}}^H)^\top$.

if (8) is solvable **then return** $\tilde{\mathbf{z}}, \tilde{\mathbf{S}}, \mathbf{E}^H$, and σ ;
else return failure.

end if
end if

$w = n + k$ and $\delta = n$, $\text{OSD}_{4-(n+k)}$ using n -ADD becomes a maximum likelihood decoder. However, increasing the order w also leads to an increase in time complexity. To address this issue, we propose an approach to reduce the problem size for OSD. Recall that OSD is used to solve a linear system with $2n$ binary variables and $n - k$ constraints. If a subset of binary variables is known, the problem size—and consequently the computational complexity—can be reduced. The number of binary variables in the reduced linear system is referred to as the *effective length* for OSD, which corresponds to the length of the remaining binary error variable vector.

We note that OSD is applied when BP fails to find a valid error that matches the syndrome. During the T iterations of message passing in BP, some coordinates become relatively more reliable than others. We have the following definition of highly reliable coordinates.

Definition 7. An error bit \mathbf{E}_i^a , where $i \in 1, \dots, n$ and $a \in X, Z$, is considered *highly reliable* if its hard-decision reliability equals T or $T + 1$, and its soft reliability $\phi^a(i)$

satisfies $\phi^a(i) \geq \theta$, where θ is a predetermined reliability threshold.

An error variable has hard reliability T if BP has a constant output at all iterations; a hard reliability of $T + 1$ means the corresponding error variable is the identity during the BP process after being initialized to the identity.

The soft reliability threshold θ is chosen close to one to ensure that a highly reliable coordinate not only exhibits an almost constant hard-decision history but also has a high soft reliability value.

These highly reliable variables are crucial in the OSD process. Identifying these variable nodes allows us to greatly reduce the computation burden of OSD.

In topological codes, such as toric or surface codes, an isolated Pauli error refers to a single-qubit Pauli error (including identity) with no neighboring nonidentity Pauli error within a radius of two qubits. These isolated Pauli errors can be decoded using BP₄ with high confidence, contributing to the highly reliable parts in the output of BP.

These highly reliable parts provide outcomes that can be trusted and will remain unchanged throughout the OSD₄ procedure with high probability. Consequently, we propose to exclude these highly reliable parts from the parity check relations. By doing so, we can avoid unnecessary calculations and prioritize our focus on the unreliable part. Our highly reliable subset reduction (HRSR) algorithm is given in Algorithm 3.

Equation (8) follows from the parity-check condition (2) as

$$\begin{aligned} \begin{bmatrix} \mathbf{z}'' \\ \mathbf{z}^H \end{bmatrix} &= \tau(\sigma(\mathbf{S}\Lambda)) [\hat{\mathbf{E}}' \quad \mathbf{E}^H]^\top \\ &= [\tilde{\mathbf{S}}(\hat{\mathbf{E}}')^\top + \mathbf{B}(\mathbf{E}^H)^\top \quad \mathbf{C}(\mathbf{E}^H)^\top] \end{aligned}$$

and using the conditions $\mathbf{z}^H = \mathbf{C}(\mathbf{E}^H)^\top$ and $\tilde{\mathbf{z}} = \mathbf{z}'' - \mathbf{B}(\mathbf{E}^H)^\top$.

If HRSR returns a reduced linear system as in (8), we then use OSD_{4-w} to solve it with hard-decision BP output \mathbf{E}' and corresponding reliabilities η , ϕ^X , and ϕ^Z . Suppose that OSD_{4-w} returns $\hat{\mathbf{E}}'$. Then the error estimate is $\sigma^{-1}([\hat{\mathbf{E}}' \quad \mathbf{E}^H])$.

Reducing the problem size may cause the reduced check matrix to lose the ability to represent all valid codewords if its dimension becomes too small. To address this, we set the soft reliability threshold θ very close to one to ensure that highly reliable bits are accurate. Furthermore, in Step 4 of Algorithm 3, we verify that the removed highly reliable bits align with the corresponding syndrome bits. If they do not, the algorithm reports a failure.

This method effectively reduces the overhead in OSD, especially at low error rates as will be shown in the simulation section. Furthermore, as the effective length in OSD is reduced, we can apply higher order OSD if only a fixed amount of computation is allowed. Consider, for instance, the case where the number of error candidates to be tested in OSD is Γ . For the original decoding problem, OSD₄₋₂ has

$$\Gamma = \binom{n+k}{0} + \binom{n+k}{1} + \binom{n+k}{2}. \quad (9)$$

Using the HRSR algorithm for v highly reliable bits, we have a reduced system of linear equations with $2n - v$

binary variables. Assume the rank of the reduced system is $n - k - (m - m')$. Then we can apply OSD_{4-w} under the constraint of Γ candidates, with w given by

$$w = \arg \max_x \sum_{i=0}^x \binom{n+k-v+(m-m')}{i} \leq \Gamma. \quad (10)$$

Note that even though the number of tested candidates is fixed, the complexity of OSD following the HRSR algorithm is lower due to the reduced effective length.

V. APPROXIMATE DEGENERATE OSD

In this section, we discuss how degeneracy in quantum codes helps reduce the computation of OSD. Recall that in OSD- w , $\sum_{i=0}^w \binom{n+k}{i}$ candidates are generated, and the one that is optimal with respect to δ -ADD is chosen as the output. As shown in Lemma 6, a new candidate can be generated from an error candidate by flipping a bit in the reliable subset and adding a certain vector to the unreliable subset. This new candidate must belong to the same error coset, and thus the bit flipping in the reliable subset corresponds to an operator in the normalizer group. We have the following degenerate error candidate pruning conditions.

Lemma 8. Consider an $[[n, k, d]]$ stabilizer code with a check matrix given by $[\mathbf{I}_{n-k} \quad \mathbf{A}]$ after Gaussian elimination and a column permutation as in Equation (3), where $\mathbf{A} \in \{0, 1\}^{(n-k) \times (n+k)}$ are associated with the reliable bits of OSD₄₋₀ output.

1) When using n -ADD, only the reliable bits corresponding to nontrivial logical operators need to be considered in OSD_{4-w}.

2) If each error corresponding to flipping a reliable bit of OSD₄₋₀ output is a stabilizer, then OSD_{4-w} is equivalent to OSD₄₋₀ for any w .

Proof. 1)

In optimal degenerate decoding (n -ADD), different stabilizer cosets are compared. Therefore, multiplying a stabilizer by an error candidate does not create a new nontrivial candidate.

2) The statement is straightforward, as flipping these reliable bits results in only degenerate errors to the OSD₄₋₀ output. \square

Exploiting Lemma 8-1) with n -ADD makes OSD_{4-w} more effective. By incorporating with the HRSR algorithm, we can work on a shortened check matrix $\tilde{\mathbf{S}}$ and higher order of OSD can be executed. Consequently, (10) can be improved to $w = \arg \max_x \sum_{i=0}^x \binom{u}{i} \leq \Gamma$, where $u \leq n+k-v+(m-m')$ is the number of columns in the shortened check matrix corresponding to nontrivial logical operators.

For checking whether flipping a bit is nontrivial can be done by checking whether its induced error anticommutes with the permuted logical operators. If an error commutes with all logical operators, it belongs to the stabilizer group. This aligns with the standard procedure in QEC simulations for calculating the logical error rate. We note that the computational complexity of verifying such a bit-flipping event is $O((n-k)k)$. Consequently, checking all the columns of

A has a computational complexity of roughly the same order as Gaussian elimination. This approach is both effective and relatively efficient for implementing high-order OSD. \square

However, the complexity of n -ADD is not practically feasible. We propose to use δ -ADD by choosing δ as the highest weight of a set of low-weight stabilizer generators. For the case of a rotated surface code [24], the stabilizer generators are of weight 2 or 4, and the next lowest stabilizer weight is 6. Thus, n -ADD can be well approximated by 4-ADD at error rates lower than 1%. Assume that OSD4-0 generates a list of error candidates \mathcal{E} . Then, 4-ADD outputs:

$$\hat{\mathbf{E}} = \arg \max_{\mathbf{E}} \sum_{i=0}^{n-k} \Pr \{ \mathbf{E} + \mathbf{S}_i \}, \quad (11)$$

where $\mathbf{S}_0 = I$ and $\{\mathbf{S}_i\}_{i=1}^{n-k}$ is a set of stabilizer generators for the rotated surface code. For practical implementation, let $W(x)$ be the (Pauli) weight enumerator of the set $\{\mathbf{E} + \mathbf{S}_i : i = 0, \dots, n-k\}$, and then the calculation of (11) can be approximated by using the dominating terms in $W(\epsilon/(1-\epsilon))$ for error rate $\epsilon < 1\%$.

For codes with algebraic structures, the first few lowest-weight terms can be derived, but determining the complete weight enumerator for a general code is an NP-hard problem. As an alternative, we propose selecting a set of $m \geq n-k$ low-weight stabilizer generators and calculating the weight distribution of $\binom{m}{c}$ stabilizers, where c is a constant independent of n . This method provides a good approximation of the dominant terms for practical purposes. To maintain an overall complexity of $O(n^3)$, the value of $\binom{m}{c}$ should be chosen accordingly.

To achieve optimal execution complexity, 0-ADD is often used. Lemma 8 suggests focusing on the columns of A corresponding to nontrivial logical operators when n -ADD is used. However, in the scenario of 0-ADD, a stabilizer may influence the output of OSD $_4$ - w since multiplying a stabilizer can reduce the weight of the error, potentially providing a better candidate in 0-ADD, even though the error coset remains unchanged. Thus, OSD $_4$ - w cannot simply flip bits corresponding to those nontrivial logical operators as in the case of Lemma 8-1).

The following provides a sufficient condition to determine whether flipping a reliable bit corresponds to a stabilizer.

Lemma 9. Consider an $[[n, k, d]]$ stabilizer code with a check matrix given by $[\mathbf{I}_{n-k} \ \mathbf{A}]$ after Gaussian elimination and a column permutation as in Equation (3), where $\mathbf{A} \in \{0, 1\}^{(n-k) \times (n+k)}$ are associated with the reliable bits of OSD $_4$ -0 output. If the weight of the j -th column of \mathbf{A} is less than $d-1$, then flipping the j -th reliable bit of an error candidate corresponds to multiplying the error candidate by a stabilizer.

Proof. Suppose that $\mathbf{E} = [\mathbf{F} \mid \mathbf{E}_1^R \ \mathbf{E}_2^R \ \dots \ \mathbf{E}_{n+k}^R]$ is a valid error candidate, where $\mathbf{E}_i \in \{0, 1\}$ for $i = 1, \dots, n$ and $\mathbf{F} \in \{0, 1\}^{n-k}$. By (7), flipping the bit \mathbf{E}_j^T corresponds to adding \mathbf{E} by the vector $[\mathbf{A}_j^T \ 0 \dots 0 \ 1 \ 0 \dots 0] \in \{0, 1\}^{2n}$, where \mathbf{A}_j is the j -th column of \mathbf{A} . This vector corresponds to a Pauli operator of weight at most $d-1$ and, therefore, is a stabilizer since the minimum distance of the code is d .

By Lemma 8-2) and Corollary 9, we establish the following operational degenerate error candidate pruning condition.

Corollary 10. Let $\tilde{S} \in \{0, 1\}^{m' \times (2n-v)}$ be a shortened check matrix by the HRSR algorithm. Suppose that \tilde{S} can be transformed into $[\mathbf{I} \ \tilde{A}]$ after Gaussian elimination and a column permutation, where \tilde{A} is associated with the reliable bits. If all the columns of \tilde{A} are of weight less than $d-1$, then OSD $_4$ - w on the corresponding reduced linear system is equivalent to OSD $_4$ -0 for any w .

The operational degenerate error pruning condition in Corollary 10 provides a more operationally efficient method to determine whether order- w OSD for $w > 0$ is nontrivial by evaluating the weight of each column. This can be done in $O((n-k) \times (n+k))$.

If there are many highly reliable bits, the number of stabilizers associated with these bits would be high. Consequently, the shortened check matrix \tilde{S} from the HRSR algorithm will have fewer rows and lower column weights. Therefore, Corollary 10 can be applied with high probability when the error rate is low.

We combine all the aforementioned techniques into the approximate degenerate OSD (ADOSD) algorithm, as detailed in Algorithm 4, using 0-ADD. It is important to note that if decoding performance is of higher priority, δ -ADD can be utilized, and Lemma 9 can be integrated into Algorithm 4.

Algorithm 4 ADOSD $_4$

Input: check matrix $\mathbf{S} \in \{0, 1\}^{m \times 2n}$ of rank $n-k$, syndrome $\mathbf{z} \in \{0, 1\}^{m \times 1}$, BP output distributions $\{\mathbf{q}_i\}_{i=1}^n$, hard-decision reliability vector $\boldsymbol{\eta} \in \mathbb{Z}^n$, belief distributions $\{\mathbf{q}_i\}_{i=1}^n$, soft reliability threshold θ , hard-decision vector $\mathbf{E} \in \{0, 1\}^{2n}$, maximum number of OSD flips Γ , and backup OSD order w .
Output: A valid error estimate $\hat{\mathbf{E}} \in \{0, 1\}^{2n}$.

Steps:

Apply the HRSR algorithm.

if HRSR returns failure, **then**

use OSD $_4$ - w to find an error estimate $\hat{\mathbf{E}} \in \{0, 1\}^{2n}$ for the original problem, and **return** $\hat{\mathbf{E}}$;

else HRSR returns \mathbf{z}' , $\tilde{\mathbf{S}}$, \mathbf{E}^H , and σ .

if all the columns of $\tilde{\mathbf{S}}$ in reduced row echelon form have weight less than $d-1$, **then** $w \leftarrow 0$;

else determine w by (10).

end if

Use OSD $_4$ - w on \mathbf{z}' , $\tilde{\mathbf{S}}$, and the given data to find an error estimate $\hat{\mathbf{E}}' \in \{0, 1\}^{2n-v}$, and **return** $\sigma^{-1}([\hat{\mathbf{E}}' \ \mathbf{E}^H])$.

end if

Remark 11. We can incorporate the idea of checking the commutation relations with permuted logical operators for column-induced errors of weight at least d into Algorithm 4.

For instance, we first identify columns with weights less than $d-1$ and then verify the commutation relations between the permuted logical operators and the errors induced by the remaining columns.

As will be shown in Table VII, using the strategy outlined in Corollary 10, OSD-0 is applied in the majority of trials when the error rate is low.

VI. SIMULATION RESULTS

We simulate the performance of various BP+OSD schemes on LCS codes [59], GHP codes [42], [43], BB codes [55], and various 2D topological codes, including toric, rotated surface, color codes and twisted XZZX codes [22]–[26], [28], [58] (see [64, Table I]).

The decoding performance of a quantum code $\mathcal{C}(\mathcal{S})$ and its decoder is assessed through the logical error rate (LER). An error $E \in \mathcal{G}_n$ is classified as a logical error if it is a nontrivial logical operator.

The simulation parameters are as follows: The maximum number of BP iterations, T , is set to 100 unless otherwise specified. In most cases, a much smaller value of T suffices for good decoding performance due to the rapid convergence of MBP₄ [31], which typically completes in just a few iterations for codes with lengths under one thousand. For instance, as shown in Table V, When MBP₄ successfully decodes the $[[225, 1, 15]]$ rotated surface code, it requires an average of only 2.41 iterations at a depolarizing rate of $\epsilon = 3.3\%$. Furthermore, our MBP₄+ADOSD₄ scheme demonstrates robustness to variations in the maximum number of iterations, as discussed in Section VI-B.

For each data point in the plots, at least 100 logical error events are collected.

In Sections VI-D and VI-E, we first demonstrate the performance of the proposed BP+OSD schemes. Then, we analyze the execution time for these schemes in Section VI-G, illustrating the efficiency of ADOSD.

In the simulations of ADOSD₄, Γ is chosen according to (9) for the purpose of comparison with OSD-2. The soft reliability threshold is set to $\theta = 0.999995$. Based on our simulations, selecting θ within the range of 0.999 to 0.999995 results in similar performance.

For comparison, we consider the following decoders: (1) the AMBP₄ decoder [31] using a random serial schedule. (2) mOSD- (w, λ) , a partial order- w OSD approach introduced in [42], which selects $\sum_{j=0}^w \binom{\lambda}{j}$ candidates for λ less reliable bits based on the reliability metric Max. (3) the BP-OSD-CS(λ) decoder in [43]. (4) BP-GDG algorithm in [54]. These decoders are summarized in Table I.

We observe that both parallel and serial schedules in BP yield similar results for toric codes and surface codes. However, the parallel schedule outperforms the serial schedule on the $[[882, 48, 16]]$ GHP code. We believe that this is because that the parallel schedule typically results in unsettled oscillations in BP, which can be resolved by OSD, whereas the serial schedule may make premature decisions on some bits, leading to incorrect convergence in the decoding process. Therefore, we consider the parallel schedule for the following simulations. Similar observations are also made in [54], [65].

A. Optimization of the parameter α in MBP₄ for ADOSD.

In this subsection, we demonstrate how to optimize the parameters of our BP+OSD schemes using LCS codes [59]. LCS

codes are a specialized type of quantum code that combines the features of surface codes and lift-product constructions. Decoding LCS codes presents the most challenging problem among all the quantum codes considered in this paper. These codes cannot be effectively handled by our previous AMBP₄ decoder [31], even though AMBP₄ outperforms binary BP-OSD decoders [42], [43] on all other codes.

In the following, we consider the MBP₄ decoder introduced in [31] as a predecoder for OSD. MBP₄ includes a parameter α that controls the step size of message updates during BP iterations: when $\alpha < 1$, the step size is enlarged; when $\alpha > 1$, the step size is reduced. For $\alpha = 1$, MBP₄ is equivalent to the refined BP₄ in [12]. We will specify the value of α only when $\alpha \neq 1$ is used.

Thus, optimizing the choice of α is crucial. For most non-degenerate codes, $\alpha = 1$ is sufficient to achieve good decoding performance. However, for degenerate codes, selecting $\alpha > 1$ can result in more stable message passing, leading to improved OSD performance. This optimization should be performed for each specific code, although the same value of α typically applies across an entire code family.

Figure 2 demonstrates the performance of MBP₄+ADOSD₄ on the $[[175, 7, 7]]$ LCS code with various values of α . The performance of MBP₄+ADOSD₄ improves significantly and stabilizes as α increases from 1 to approximately 1.6.

For reference, we provide a curve $y = ax^4$ for some a if errors of weight up to half of the code distance $\lfloor \frac{d-1}{2} \rfloor$ can be corrected. Therefore, MBP₄+ADOSD₄ with $\alpha = 1.6$ matches this prediction around LER 10^{-7} . On the other hand, AMBP meets an earlier error floor around LER 10^{-3} .

Figure 2 also includes a curve labeled MLE (independent X/Z), which is an estimate of the maximum likelihood binary decoding performance using integer programming, as reported in [59]. Since the decoding of X and Z errors is performed independently, this MLE curve represents the optimal performance only under the assumption that X and Z errors are uncorrelated. In [59], the performance of the BP-OSD-CS decoding algorithm from [43] was shown to approximately match the MLE curve. However, it is evident that MBP₄+ADOSD₄ significantly outperforms this MLE curve.

We observe a similar performance of MBP₄+ADOSD₄ for $[[15, 3, 3]]$, $[[65, 5, 5]]$ and $[[369, 9, 9]]$ LCS codes as well, while AMBP has an even higher error floor around LER 10^{-2} for the $[[369, 9, 9]]$ LCS code and a lower error floor around 10^{-5} for the $[[65, 5, 5]]$ LCS code.

B. Robustness of the maximum iterations in MBP₄+ADOSD₄

Next, we demonstrate that the performance of ADOSD₄ remains robust even with variations in the maximum number of iterations in MBP₄. We note that in ADOSD₄, OSD- w is invoked when HRSR fails. As a result, the overall algorithm maintains high accuracy.

However, the failures of the HRSR algorithm can impact the simulation time, as OSD- w is significantly more time-consuming.

Figure 3 illustrates the performance of MBP₄+ADOSD₄ decoding with varying maximum numbers of iterations, $T =$

decoder	source	note
MBP ₄ +ADOSD ₄	this paper	based on Algorithm 4
MBP ₄ +OSD ₄ -w	this paper	order-w OSD ₄ with reliability metric from Definition 4
MBP ₄ +mOSD ₄ -w	this paper	order-w OSD ₄ with reliability metric from Definition 5
AMBP ₄	[31]	No postprocessing. Can act as a predecoder for ADOSD ₄ and OSD ₄
BP+mOSD-(w,λ)	[42]	binary BP+ order-w OSD ₄ with additional flips on λ positions
BP-OSD-CS(λ)	[43]	binary BP-OSD-0 with a greed search on $\binom{\lambda}{2}$ positions
BP+GDG	[54]	binary BP with guided decimal guessing based on a decision tree

TABLE I

VARIOUS DECODERS COMPARED IN THIS PAPER.

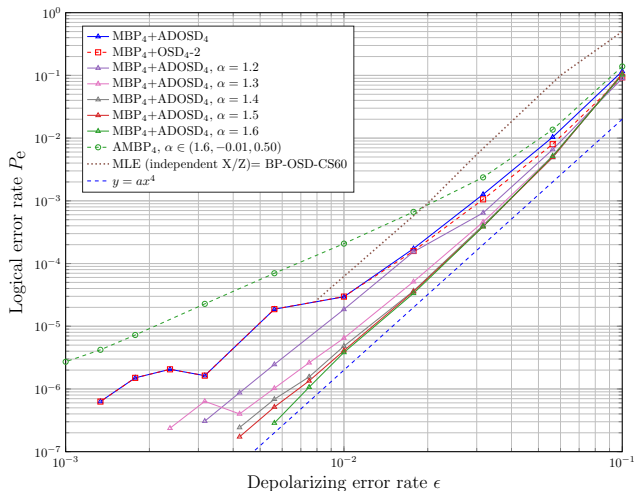


Fig. 2. MBP₄+ADOSD₄ decoding with various values of α for the $[[175, 7, 7]]$ LCS code. The curve MLE is taken from [59]. The notation $\alpha \in (1.6, -0.01, 0.5)$ means that α is tested in the sequence 1.60, 1.59, 1.58, \dots , 0.51, 0.50.

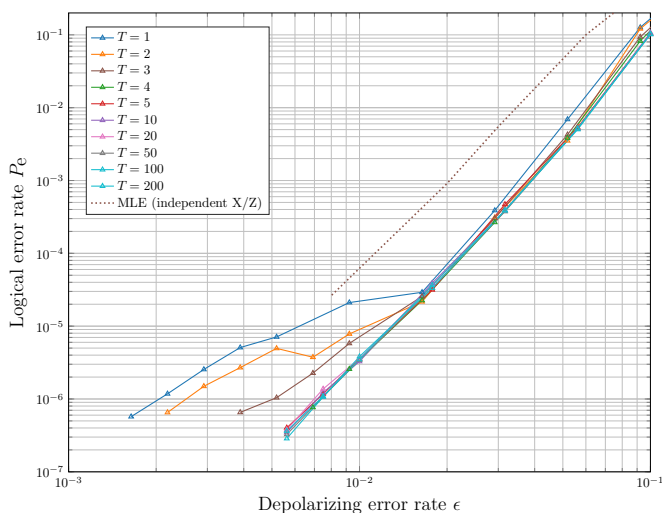


Fig. 3. MBP₄+ADOSD₄ decoding with various maximum number of iterations T for the $[[175, 7, 7]]$ LCS code.

1, 2, 3, 4, 5, 10, 20, 50, 100, 200. The curve for $T = 4$ is already good enough and smooth. While increasing the number of iterations results in slightly improved performance, the curves converge closely around an LER of 2×10^{-7} to 3×10^{-7} .

In the extreme case of $T = 1$, there are few highly reliable bits or valid highly reliable bits, causing the decoder to essentially revert to performing ordinary OSD₄ with increased complexity.

We have demonstrated that the performance of ADOSD₄ remains robust even with variations in the maximum number of iterations in MBP₄. To balance accuracy and efficiency, we typically select T within the range of 50 to 100.

C. Bivariate bicycle codes

A class of QLDPC codes, referred to as BB codes, was proposed in [55], demonstrating a high error threshold and a significantly higher code rate compared to topological codes. Several attempts at decoding this code family have been presented in [53], [54] under the code capacity noise model. However, the BP+CB decoder in [53] does not perform as well as BP-OSD-0. The BP+GDG decoder in [54] shows improved performance, surpassing BP-OSD-0 and being comparable to BP2-OSD-CS10 over independent X errors, as shown in [54, Figure 4].

Figure 4 presents the simulation results of MBP₄+ADOSD₄ and AMBP₄ decoding for BB codes, both of which demonstrate significantly better performance than GDG decoding. For instance, consider the $[[144, 12, 12]]$ BB code. At an X error rate of 0.02 (corresponding to a depolarizing rate of about 0.03), BP+GDG achieves an LER of approximately 10^{-4} . In contrast, both MBP₄+ADOSD₄ and AMBP₄ achieve an LER below 4×10^{-6} at the same depolarizing rate. Moreover, MBP₄+ADOSD₄ outperforms AMBP₄.

For the $[[144, 12, 12]]$ code, we also include the decoding performance of MBP₄+OSD₄-2, which is nearly identical to that of MBP₄+ADOSD₄.

D. Generalized hypergraph-product codes

The $[[882, 48, 16]]$ GHP code [42] is highly-degenerate, which causes conventional BP to perform poorly on this code. With minimum distance of 16, we can gauge the effectiveness of a good decoding algorithm on this GHP code.

The performance curves of different combinations of MBP and OSD are shown in Figure 5, where α is either fixed and OSD are shown in Figure 5, where α is either fixed at 1.6 or chosen by $\alpha(\epsilon)$. It is suggested in [31, Fig. 3] (arXiv version) that α and ϵ follow the relationship $\alpha(\epsilon) =$

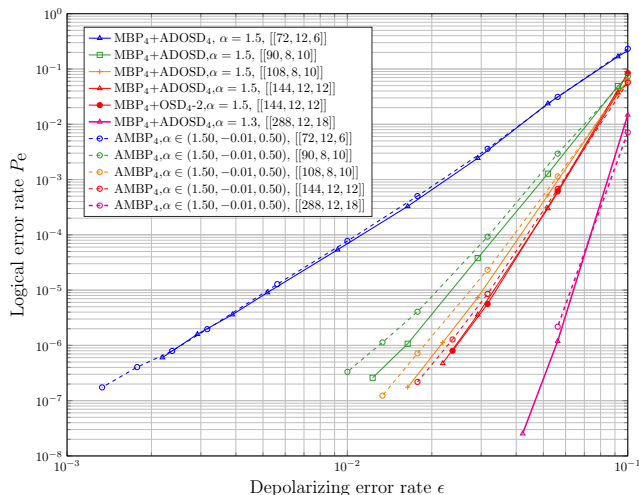


Fig. 4. AMBP₄ and MBP₄+ADOSD₄ decoding performance for various BB codes.

$-0.16 \log_{10}(\epsilon) - 0.48$, with the coefficients -0.16 and -0.48 determined through pre-simulations on the $[[882, 48]]$ code. For comparison, we also plot the performance of AMBP₄ [31] and the BP+mOSD- (w, λ) [42].

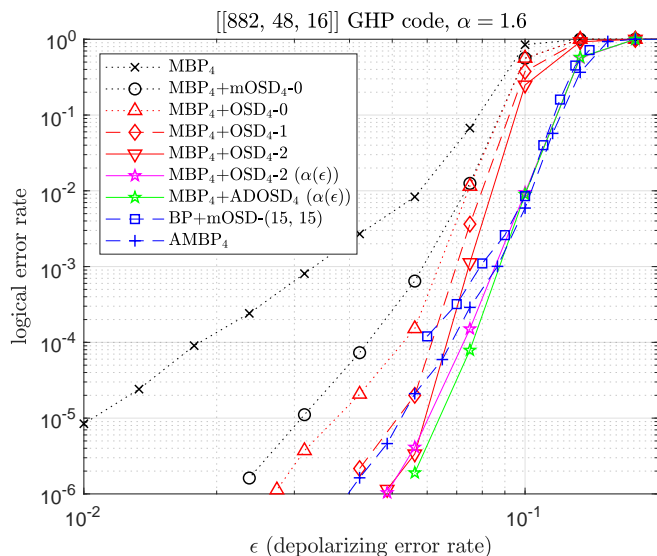


Fig. 5. Comparison of various BP-OSD schemes on the $[[882, 48]]$ GHP code. The curve BP+mOSD-(15,15) is from [42].

The results are summarized as follows.

- 1) MBP₄ can be greatly enhanced by OSD.
- 2) MBP₄+OSD₄-0 outperforms MBP₄+mOSD₄-0 (without hard-decision reliability) by roughly half an order of performance. This suggests that the hard-decision history of BP is crucial in determining the reliability order.
- 3) MBP₄+ADOSD₄ performs slightly better than MBP₄+OSD₄-2, while also reducing the time consumption, as shown in Table IV in Section VI-G.
- 4) Both MBP₄+ADOSD₄ and MBP+OSD₄-2 improve upon BP+mOSD-(15, 15) [42] by more than an order of mag-

nitude at $\epsilon = 0.05$. Note that mOSD-(15, 15) essentially enumerates all the 15 less reliable bits.

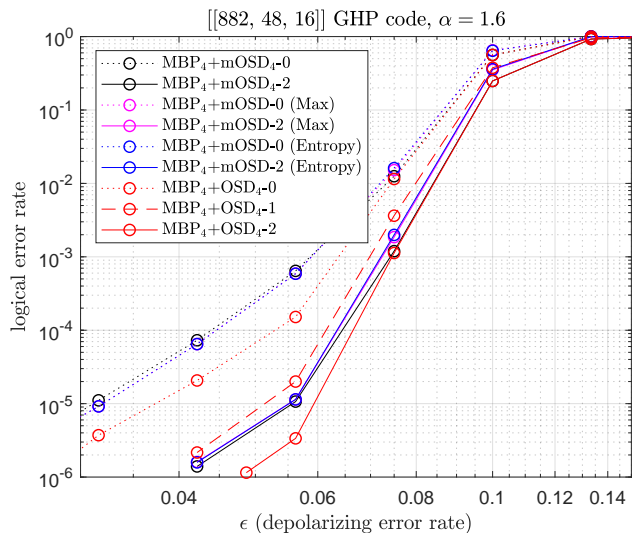


Fig. 6. Comparison of various metrics for reliability order in MBP₄-OSD₄ on the $[[882, 48, 16]]$ GHP code.

In this paper, we propose using integrated hard-decision and soft reliabilities as a reliability metric (Definition 4). Herein we also simulate the performances of MBP₄+mOSD based on the reliability metrics of Entropy or Max as shown in Figure 6, including mOSD₄ as well. Two conclusions are as follows:

- 1) The reliability metric in Definition 4, which incorporates historical message information, outperforms other metrics that rely solely on the last belief distributions.
- 2) The performances of mOSD based on Definition 5, Entropy, or Max are mostly comparable; mOSD- w based on Definition 5 is slightly better than the other two metrics at lower error rate for $w = 2$.

We have conducted additional simulations on a $[[625, 25, 8]]$ GHP code [43], as shown in Figure 7. In these examples, MBP₄+ADOSD₄ slightly outperforms both AMBP₄ and MBP₄+OSD₄-2, with all three decoders performing significantly better than BP-OSD-CS60 in [43].

E. 2D topological codes

Next, we consider the decoding performance of our BP+OSD schemes on various 2D topological codes. Since AMBP₄ is also capable of decoding various families of topological codes, it serves as a useful reference for evaluating the performance of the BP+OSD approach. It is important to examine the decoding performance when the logical error rate is around 10^{-6} , as this can reveal whether an iterative decoder exhibits an error floor behavior.

Figure 8 illustrates the performance curves of MBP₄+ADOSD₄ and AMBP₄ on the (4.8.8) color codes with distances ranging from 3 to 17. The results show that MBP₄+ADOSD₄ using $\alpha = 1.6$ improves AMBP₄ starting from $d = 5$.

The advantages of our BP+OSD schemes over AMBP₄ are also evident in rotated toric, rotated surface, XZZX,

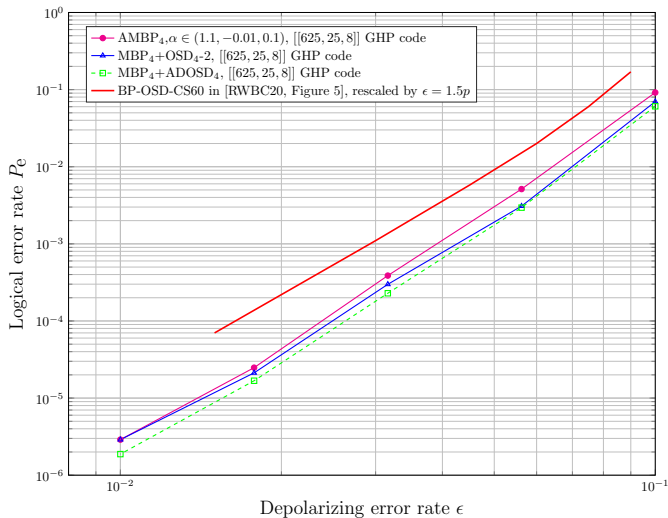


Fig. 7. Decoding performance of the $[[625,25,8]]$ GHP code. Note that the performance curve for BP-OSD-CS60 is taken from [43, Figure 5], with its independent X/Z error rate p rescaled by a factor of 1.5 to approximate depolarizing error performance.

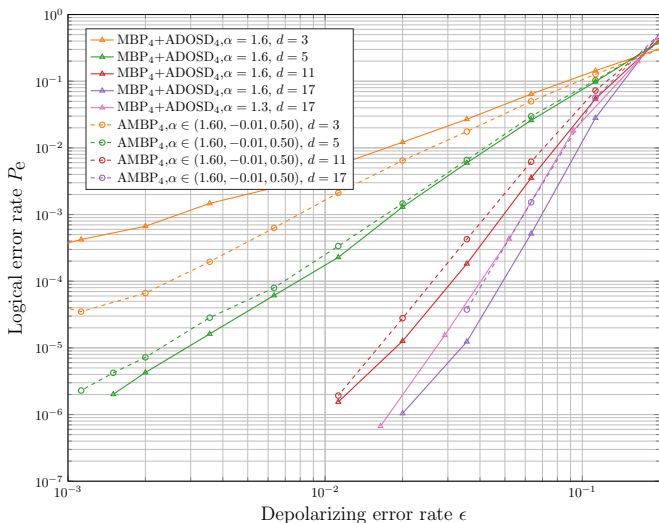


Fig. 8. $AMBP_4$ vs. MBP_4+OSD_4-2 on the (4.8.8) color codes.

and (6.6.6) color codes. Additionally, MBP_4+OSD_4-2 and $MBP_4+ADOSD_4$ exhibit nearly identical performance on these codes.

To sum up, $ADOSD_4$ and OSD_4-2 exhibit nearly identical performances on toric, surface, and twisted XZZX codes, with OSD_4-2 performing slightly better on the (6.6.6) and (4.8.8) color codes. The threshold analysis for these codes in the next subsection will reflect these results as well. We remark, however, the time consumption for $ADOSD_4$ is significantly lower than that for OSD_4-2 , as will be shown in Section VI-G.

F. Threshold analysis for the topological codes

The decoding performance of a family of 2D topological codes is typically evaluated by its simulated error threshold, which can be estimated using the scaling ansatz method [66], [67], which is explained as follows.

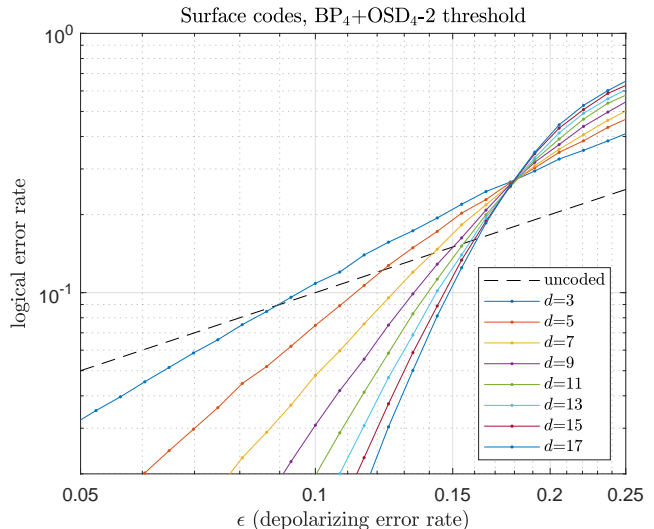


Fig. 9. The threshold of BP_4+OSD_4-2 on the surface codes is about 17.67% from the simulations. The dashed line stands for no error correction.

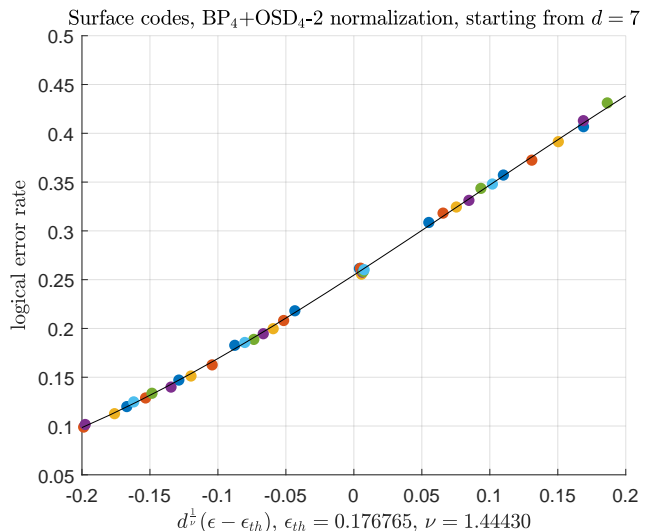


Fig. 10. The accuracy of the threshold estimation about MBP_4+OSD_4-2 on the rotated surface codes can be demonstrated using the critical scaling approach. The estimation process begins with $d = 7$ and continues up to $d = 17$, ensuring that no biased information influences the results.

Suppose that the threshold value of a code family is ϵ_{th} . For a code in this family of distance d , if the logical error rate is p_L at physical error rate ϵ , then

$$p_L = f(d^{1/\nu}(\epsilon - \epsilon_{th})), \quad (12)$$

where f is a low-degree polynomial and ν is the critical exponent. The scaling ansatz method involves fitting this equation with the best values of ϵ_{th} , ν , and f .

The threshold analysis for rotated surface codes is presented in Figure 9 and Figure 10. For each data point, we collected at least 10,000 logical error events. The analysis reveals a threshold of approximately 17.67% for BP_4+OSD_4-2 on surface codes. Similar analyses are conducted for toric, twisted XZZX, (6.6.6), and (4.8.8) color codes, using both BP_4+OSD_4-2 and

TABLE II
THRESHOLDS FOR 2D TOPOLOGICAL CODES SUBJECTE TO DEPOLARIZING ERRORS. THE PARAMETER FOR MBP₄ IS SET TO $\alpha = 1.0$.

code family	MBP ₄ +OSD ₄ -2	MBP ₄ +ADOSD ₄	AMBP ₄
rotated toric	17.52%	17.52%	≈ 17.5%
rotated surface	17.67%	17.67%	≈ 16%
(6.6.6) color	15.41%	15.18%	≈ 14.5%
(4.8.8) color	15.09%	14.69%	≈ 14.5%
XZZX twisted	17.72%	17.72%	≈ 17.5%

TABLE III
THRESHOLDS OF SEVERAL DECODERS OVER DEPOLARIZING ERRORS.

decoder	threshold
BP ₂ +mOSD-(2,60) [43]	14.85% (toric codes)*
MWPM [68], [69]	15.5% (toric codes)
AMBP ₄ [31]	17.5% (toric codes)
BP ₄ +OSD ₄ -2 (this paper)	17.52% (toric codes)

*: estimated from the threshold of 9.9% in the bit-flip channel [43].

BP₄+ADOSD₄. In the simulations, the data is fitted using a low-degree polynomial.

Note that MBP₄ with $\alpha = 1$ is used in the threshold analyses. Optimizing the value of $\alpha(\epsilon)$ for MBP can enhance overall performance.

The summarized results, including thresholds obtained with AMBP₄, are shown in Table II. These results are consistent with the simulations in the previous subsection. Notably, BP₄+OSD₄-2 shows a significant enhancement over AMBP₄ for surface and color codes.

We also compare the thresholds of our decoder with those of other known decoders in Table III, including minimum-weight perfect matching (MWPM) [68], [69]. In [43], BP₂+mOSD-(2,60) achieved a threshold of $p = 9.9\%$ on toric codes for bit-flip errors. We estimate that it has a threshold of $\epsilon_{th} = 9.9\% \times \frac{3}{2} = 14.85\%$ for depolarizing errors [1].

G. Time consumption

TABLE IV
COMPARISON OF THE TIME CONSUMPTION BETWEEN ADOSD₄ AND OSD₄-2 AT LOGICAL ERROR RATE ABOUT 2×10^{-6} .

Code	BP failure rate	ADOSD ₄ time (μ s)	OSD ₄ -2 time (μ s)	time* ratio	LER [†] ratio
toric	27.76%	88.63	4712.9	1.88%	≈ 0dB
surface	67.69%	71.97	3549	2.82%	≈ 0dB
(6.6.6)	10.32%	35.42	3812	0.93%	-2.3dB
(4.8.8)	7.17%	26.50	1265	2.09%	-3.9dB
XZZX	11.93%	22.29	1001.3	2.23%	≈ 0dB
GHP	0.86%	1188.7	45910.3	2.59%	2.49dB

*: the column ‘time ratio’ represents the ratio of MBP₄+ADOSD₄ time to OSD₄-2 time.

†: the column ‘LER ratio’ represents the ratio of the logical error rate using ADOSD₄ to that using OSD₄-2. If the LER ratio is greater than 0dB, it means that ADOSD₄ is better.

In the previous subsections, we have demonstrated the effectiveness of our BP+OSD schemes. In this subsection we analyze the time efficiency of our OSD schemes.

1) *Time Consumption of ADOSD₄ vs. OSD₄-2*: First, we compare the time consumption of OSD₄-2 and ADOSD₄ for various topological codes of comparable distances with the [[882, 48, 16]] GHP code, including the [[324, 2, 18]] rotated toric code, the [[289, 1, 17]] rotated surface code, the [[217, 1, 17]] (6.6.6) color code, the [[161, 1, 17]] (4.8.8) color code, and the [[145, 1, 17]] twisted XZZX code. For each code, the simulated physical error rate is chosen so that the logical error rate of MBP₄+ADOSD₄ is approximately 2×10^{-6} . We fix $\alpha = 1$ in this subsection and the decoding performance can be further improved.

In the simulations, when BP fails, the BP outputs will be handled by ADOSD₄ and OSD₄-2, respectively. We note that ADOSD₄ is invoked only when MBP₄ fails. and their time consumption statistics will be counted separately in the following tables. For example, ADOSD₄ time only counts the time to run Algorithm 4 when MBP₄ fails.

The simulation results are summarized in Table IV and the unit of time is microseconds (μ s) measured using a single-thread desktop computer. It can be observed that the time consumption of ADOSD₄ is roughly 1% to 3% of the time consumption for OSD₄-2 at logical error rate about 2×10^{-6} for the various quantum codes.

For the toric, surface, and twisted XZZX codes, ADOSD₄ and OSD₄-2 exhibit almost identical performances, while OSD₄-2 performs better on the color codes and ADOSD₄ performs better on the GHP code. This is reflected in the last column of Table IV.

To summarize, ADOSD₄ is at least 30 times faster than OSD₄-2, with a maximum performance loss of 4dB for topological codes at logical error rate 2×10^{-6} . Additionally, for the [[882, 48]] GHP code, ADOSD₄ also enhances performance.

2) *Time Consumption of ADOSD₄ vs. BP*: We have demonstrated that ADOSD₄ is generally faster than OSD₄-2. Next, we compare the time consumption of ADOSD₄ to MBP₄, using surface codes.

TABLE V
COMPARISON OF THE TIME CONSUMPTION FOR SURFACE CODES AT LOGICAL ERROR RATE ABOUT 10^{-6} .

code distance	average iterations*	time per MBP ₄ iteration (μ s)	MBP ₄ failure rate	time per ADOSD ₄ (μ s)	time per OSD ₄ -2 (μ s)
11	22.3473	0.01464	21.46%	0.0272	0.667
13	37.1148	0.0212	35.97%	0.0469	1.342
15	52.6400	0.0287	51.47%	0.0506	2.155

*: average over all samples, including MBP failures.

TABLE VI
TIME CONSUMPTION OF ADOSD₄ VS. BP FOR THE SURFACE CODES

code distance	ϵ	average iterations [†] when MBP ₄ succeeds	ADOSD ₄ time in MBP ₄ iterations
11	1.7%	1.002	2
13	2.5%	1.79	2.21
15	3.3%	2.41	1.76

†: average over only the samples when MBP₄ succeeds.

Table V lists the time consumptions of MBP₄, ADOSD₄, and OSD₄-2 for surface codes with distances of 11, 13, and 15. To achieve a logical error rate 10^{-6} using ADOSD₄, the physical error rates are set to 0.017, 0.025, and 0.033 for codes with distances 11, 13, and 15, respectively. At least 10^5 samples are collected for each case. For example, at $d = 11$, the MBP₄ failure rate is 21.46% at physical error rate 1.7%. Since the maximum number of iterations is set to be $T = 100$, this contributes to an average of 21.46 iterations. Since the average iterations include MBP₄ failures is 22.3473, the average iterations when MBP₄

Table VI summarizes the time consumption of ADOSD₄ in terms of MBP₄ iterations. Specifically, the average time consumption per codeword for ADOSD₄ is approximately equivalent to 1.76 to 2.21 MBP₄ iterations. This shows that the time consumption for ADOSD₄ is roughly equivalent to 1 to 2 successful MBP₄ executions. Furthermore, the time usage for ADOSD₄ is significantly smaller than OSD₄-2.

3) *HRSR and OSD-0 in ADOSD₄*: We have shown that ADOSD₄ is efficient, thanks to Algorithm 3 and Corollary 10. These methods reduce the effective length using reliable subset reduction and allow us to perform only OSD₄-0 by identifying degenerate error cosets. Now, we examine the effectiveness of these techniques on the surface code of distance 11, with similar results observed for distances 13 and 15.

Table VII enumerates the percentage of ADOSD₄ trials that only perform OSD₄-0 using Corollary 10. At $\epsilon = 4.1\%$, 93.61% of ADOSD₄ trials already perform only OSD₄-0, increasing to 99.84% at $\epsilon = 1.7\%$. Thus, at lower error rates, almost all trials execute OSD₄-0.

Moreover, the HRSR algorithm effectively reduces the dimensions of the check matrix in both rows and columns. Table VII also provides the percentages of trials where the number of rows and columns in the check matrix is reduced to 20% or 30% of the original (denoted as 20% and 30% effective dimensions in the table). These percentages increase quickly as the error rate decreases. With fewer than 30% effective dimensions, the time consumption for Gaussian elimination reduces to roughly $0.3^3 = 2.7\%$, consistent with the results in Table IV.

TABLE VII
PERCENTAGE OF OSD-0 IN ADOSD₄ ON THE SURFACE CODE OF
DISTANCE 11

depolarizing rate ϵ	1.7%	2.7%	4.1%
LER	10^{-6}	10^{-5}	10^{-4}
OSD-0	99.84%	98.85%	93.61%
20% effective dimensions	44.13%	26.30%	5.13%
30% effective dimensions	94.04%	84.46%	57.91%

VII. CONCLUSION

We proposed quaternary OSD with integrated hard- and soft-decision reliabilities to retain the X/Z correlations. Our BP-OSD schemes have demonstrated highly effective decoding capabilities for various sparse quantum codes in the code capacity noise model, including both CSS and non-CSS

codes. Additionally, when the logical error rate is around 10^{-6} , ADOSD₄ can further enhance the decoding process by offering accelerated decoding while maintaining comparable performance. As a result, ADOSD₄ is applicable to small or medium-sized codes with $n \approx 1000$, significantly enhancing the performance of BP in the code capacity noise model. In our simulations, we restricted the number of error candidates to the size of order-2 OSD; better performance of ADOSD₄ can be achieved by allowing for greater options.

We note that while all the techniques developed in this paper are presented in the context of quaternary error variables, they can naturally be adapted to binary OSD for handling CSS codes. This includes hard-decision reliability, highly reliable subset reduction, approximate degenerate decoding, and degenerate candidate pruning conditions, by restricting the approach to either X - or Z -stabilizers. Furthermore, these techniques can be integrated with other methods available in the literature.

Although the intention of [56] and [57] is quite similar to our HRSR algorithm, the underlying approaches differ: their methods focus on dividing the decoding problem into several smaller problems, whereas our approach involves simply removing the most reliable bits. Consequently, it may be possible to combine their methods with ours. For example, apply HRSR first, followed by either of the algorithms.

In our investigations, we primarily focused on MBP₄+OSD₄-2 and ADOSD₄. However, MBP₄+OSD₄-0 has also exhibited excellent performance for most codes, aligning with the findings in [42]. In particular, we found that ADOSD₄ mostly performs only MBP₄+OSD₄-0 at low error rates. On the other hand, at low error rates (e.g., below 10^{-3}), there are small non-isolated errors, so the effective length for OSD is relatively small, allowing us to perform higher-order OSD. We have observed some instances of surface codes with order w up to 13 in (9).

An interesting observation is that we can identify bit-flips in error candidates corresponding to multiplying a stabilizer operator, as stated in Lemma 8 and Corollary 10. This information can be used to improve the algorithm by flipping effective bits in approximate degenerate decoding. Additionally, another potential improvement is extending the candidate pruning condition by Fossorier *et al.* [46] to quantum codes.

We chose the binary representation of quantum codes and syndrome correction for developing the OSD algorithm. A quantum code can be interpreted as a quaternary additive code with binary error syndromes [5]. Thus, one might consider formulating a system consisting of n quaternary variables and $n - k$ additive constraints and employ a Gaussian elimination process for quaternary additive groups. However, for practical implementation, we chose to binarize this process.

There are various reliability metrics that consider the (weighted) accumulation of the log-likelihood ratio (LLR) signs for each bit during BP iterations [70]–[73]. Our hard-decision reliability can be viewed as an extension of this idea, focusing on the length of the last run in the hard-decision vectors. The reliability order in Definition 4 can be adapted to employ alternative metrics, such as Entropy or Max. From our experiments, the integrated hard- and soft-decision reliabilities

yielded the best results.

Finally, our BP-OSD scheme can be extended to handle both data and syndrome errors in the phenomenological noise model [74], [75], using techniques proposed in [76]–[78], or to the circuit-level noise model [79], as demonstrated in our recent work [78].

Currently, there is significant progress in circuit-level error decoding [55], [80]–[82]. Various decoders have been shown to work for circuit-level noise models, including BP-OSD-CS [43], guided decimal guessing (GDG) [54], ambiguity clustering [56], localized statistics decoding (LSD) [57], and ordered Tanner forest (OTF) [83]. These decoders are based on detector error models generated by STIM [84] and utilize binary BP combined with postprocessing.

However, there are several code capacity error decoding problems where BP-OSD is suboptimal, indicating potential for further improvement in the circuit-level noise model. Therefore, we aim to extend our BP+OSD method to address these more demanding scenarios effectively.

REFERENCES

- [1] C.-F. Kung, K.-Y. Kuo, and C.-Y. Lai, “On belief propagation decoding of quantum codes with quaternary reliability statistics,” in *2023 12th International Symposium on Topics in Coding (ISTC)*, 2023, pp. 1–5.
- [2] B. M. Terhal, “Quantum error correction for quantum memories,” *Reviews of Modern Physics*, vol. 87, no. 2, pp. 307–346, 2015.
- [3] C.-Y. Lai and K.-Y. Kuo, “Harnessing coding theory for reliable network quantum communication,” *IEEE Wireless Communications*, vol. 31, no. 4, pp. 82–88, 2024.
- [4] D. Gottesman, “Stabilizer codes and quantum error correction,” Ph.D. dissertation, Caltech, 1997.
- [5] A. R. Calderbank, E. M. Rains, P. W. Shor, and N. J. A. Sloane, “Quantum error correction via codes over GF(4),” *IEEE Trans. Inf. Theory*, vol. 44, no. 4, pp. 1369–1387, 1998.
- [6] M. A. Nielsen and I. L. Chuang, *Quantum Computation and Quantum Information*. Cambridge University Press, 2000.
- [7] D. J. C. MacKay, G. Mitchison, and P. L. McFadden, “Sparse-graph codes for quantum error correction,” *IEEE Trans. Inf. Theory*, vol. 50, no. 10, pp. 2315–2330, 2004.
- [8] D. Poulin and Y. Chung, “On the iterative decoding of sparse quantum codes,” *Quantum Inf. Comput.*, vol. 8, pp. 987–1000, 2008.
- [9] Y.-J. Wang, B. C. Sanders, B.-M. Bai, and X.-M. Wang, “Enhanced feedback iterative decoding of sparse quantum codes,” *IEEE Trans. Inf. Theory*, vol. 58, no. 2, pp. 1231–1241, 2012.
- [10] Z. Babar, P. Botsinis, D. Alanis, S. X. Ng, and L. Hanzo, “Fifteen years of quantum LDPC coding and improved decoding strategies,” *IEEE Access*, vol. 3, pp. 2492–2519, 2015.
- [11] A. Rigby, J. C. Olivier, and P. Jarvis, “Modified belief propagation decoders for quantum low-density parity-check codes,” *Phys. Rev. A*, vol. 100, no. 1, p. 012330, 2019.
- [12] K.-Y. Kuo and C.-Y. Lai, “Refined belief propagation decoding of sparse-graph quantum codes,” *IEEE J. Sel. Areas Inf. Theory*, vol. 1, no. 2, pp. 487–498, 2020.
- [13] C.-Y. Lai and K.-Y. Kuo, “Log-domain decoding of quantum LDPC codes over binary finite fields,” *IEEE Trans. Quantum Eng.*, vol. 2, 2021, article no. 2103615.
- [14] R. G. Gallager, “Low-density parity-check codes,” *IRE Trans. Inf. Theory*, vol. 8, no. 1, pp. 21–28, 1962.
- [15] D. J. C. MacKay and R. M. Neal, “Good codes based on very sparse matrices,” in *Proc. IMA Int. Conf. Cryptogr. Coding*, 1995, pp. 100–111.
- [16] D. MacKay, “Good error-correcting codes based on very sparse matrices,” *IEEE Trans. Inf. Theory*, vol. 45, no. 2, pp. 399–431, 1999.
- [17] R. Tanner, “A recursive approach to low complexity codes,” *IEEE Trans. Inf. Theory*, vol. 27, no. 5, pp. 533–547, 1981.
- [18] J. Pearl, *Probabilistic reasoning in intelligent systems: networks of plausible inference*. Kaufmann, 1988.
- [19] F. R. Kschischang, B. J. Frey, and H.-A. Loeliger, “Factor graphs and the sum-product algorithm,” *IEEE Trans. Inf. Theory*, vol. 47, no. 2, pp. 498–519, 2001.
- [20] A. R. Calderbank and P. W. Shor, “Good quantum error-correcting codes exist,” *Phys. Rev. A*, vol. 54, p. 1098, 1996.
- [21] A. M. Steane, “Error correcting codes in quantum theory,” *Phys. Rev. Lett.*, vol. 77, p. 793, 1996.
- [22] A. Y. Kitaev, “Fault-tolerant quantum computation by anyons,” *Annals of Physics*, vol. 303, no. 1, pp. 2–30, 2003.
- [23] H. Bombin and M. A. Martin-Delgado, “Topological quantum distillation,” *Phys. Rev. Lett.*, vol. 97, no. 18, p. 180501, 2006.
- [24] H. Bombin and M. A. Martin-Delgado, “Optimal resources for topological two-dimensional stabilizer codes: Comparative study,” *Phys. Rev. A*, vol. 76, no. 1, p. 012305, 2007.
- [25] C. Horsman, A. G. Fowler, S. Devitt, and R. Van Meter, “Surface code quantum computing by lattice surgery,” *New J. Phys.*, vol. 14, no. 12, p. 123011, 2012.
- [26] B. Terhal, F. Hassler, and D. DiVincenzo, “From Majorana fermions to topological order,” *Phys. Rev. Lett.*, vol. 108, no. 26, p. 260504, 2012.
- [27] A. J. Landahl, J. T. Anderson, and P. R. Rice, “Fault-tolerant quantum computing with color codes,” *arXiv preprint arXiv:1108.5738*, 2011.
- [28] J. Bonilla Ataides, D. Tuckett, S. Bartlett, S. Flammia, and B. Brown, “The XZZX surface code,” *Nat. Commun.*, vol. 12, no. 1, pp. 1–12, 2021.
- [29] N. Raveendran and B. Vasić, “Trapping sets of quantum LDPC codes,” *Quantum*, vol. 5, p. 562, 2021.
- [30] D. Chytas, M. Pacenti, N. Raveendran, M. F. Flanagan, and B. Vasić, “Enhanced message-passing decoding of degenerate quantum codes utilizing trapping set dynamics,” *IEEE Communications Letters*, vol. 28, no. 3, pp. 444–448, 2024.
- [31] K.-Y. Kuo and C.-Y. Lai, “Exploiting degeneracy in belief propagation decoding of quantum codes,” *npj Quantum Inf.*, vol. 8, 2022, article no. 111. [Online]. Available: <https://arxiv.org/abs/2104.13659>
- [32] M. P. Fossorier and S. Lin, “Soft-decision decoding of linear block codes based on ordered statistics,” *IEEE Trans. Inf. Theory*, vol. 41, no. 5, pp. 1379–1396, 1995.
- [33] J. Wolf, “Efficient maximum likelihood decoding of linear block codes using a trellis,” *IEEE Trans. Inf. Theory*, vol. 24, no. 1, pp. 76–80, 1978.
- [34] A. Lafourcade and A. Vardy, “Asymptotically good codes have infinite trellis complexity,” *IEEE Trans. Inf. Theory*, vol. 41, no. 2, pp. 555–559, 1995.
- [35] P. Elias, “List decoding for noisy channels,” in *IRE WESCON Conv. Rec.*, 1957, pp. 94–104.
- [36] —, “Error-correcting codes for list decoding,” *IEEE Trans. Inf. Theory*, vol. 37, no. 1, pp. 5–12, 1991.
- [37] G. Forney, “Generalized minimum distance decoding,” *IEEE Trans. Inf. Theory*, vol. 12, no. 2, pp. 125–131, 1966.
- [38] D. Chase, “Class of algorithms for decoding block codes with channel measurement information,” *IEEE Trans. Inf. Theory*, vol. 18, no. 1, pp. 170–182, 1972.
- [39] J. Snyders and Y. Be’ery, “Maximum likelihood soft decoding of binary block codes and decoders for the Golay codes,” *IEEE Trans. Inf. Theory*, vol. 35, no. 5, pp. 963–975, 1989.
- [40] T. Kaneko, T. Nishijima, H. Inazumi, and S. Hirasawa, “An efficient maximum-likelihood-decoding algorithm for linear block codes with algebraic decoder,” *IEEE Trans. Inf. Theory*, vol. 40, no. 2, pp. 320–327, 1994.
- [41] Y. S. Han, C. R. Hartmann, and C.-C. Chen, “Efficient priority-first search maximum-likelihood soft-decision decoding of linear block codes,” *IEEE Trans. Inf. Theory*, vol. 39, no. 5, pp. 1514–1523, 1993.
- [42] P. Pantelev and G. Kalachev, “Degenerate quantum LDPC codes with good finite length performance,” *Quantum*, vol. 5, p. 585, 2021. [Online]. Available: <https://arxiv.org/abs/1904.02703>
- [43] J. Roffe, D. R. White, S. Burton, and E. Campbell, “Decoding across the quantum low-density parity-check code landscape,” *Phys. Rev. Res.*, vol. 2, no. 4, p. 043423, 2020.
- [44] M. Fossorier, “Iterative reliability-based decoding of low-density parity check codes,” *IEEE Journal on Selected Areas in Communications*, vol. 19, no. 5, pp. 908–917, 2001.
- [45] M. Baldi, F. Chiaraluce, N. Maturò, G. Liva, and E. Paolini, “A hybrid decoding scheme for short non-binary LDPC codes,” *IEEE Communications Letters*, vol. 18, no. 12, pp. 2093–2096, 2014.
- [46] M. P. Fossorier, S. Lin, and J. Snyders, “Reliability-based syndrome decoding of linear block codes,” *IEEE Trans. Inf. Theory*, vol. 44, no. 1, pp. 388–398, 1998.
- [47] M. P. Fossorier and S. Lin, “Computationally efficient soft-decision decoding of linear block codes based on ordered statistics,” *IEEE Trans. Inf. Theory*, vol. 42, no. 3, pp. 738–750, 1996.

- [48] D. Gazelle and J. Snyders, "Reliability-based code-search algorithms for maximum-likelihood decoding of block codes," *IEEE Trans. Inf. Theory*, vol. 43, no. 1, pp. 239–249, 1997.
- [49] S. E. Alnawayseh and P. Loskot, "Ordered statistics-based list decoding techniques for linear binary block codes," *EURASIP J. Wireless Commun. Netw.*, vol. 2012, pp. 1–12, 2012.
- [50] C. Yue, M. Shirvanimoghaddam, Y. Li, and B. Vucetic, "Segmentation-discarding ordered-statistic decoding for linear block codes," in *IEEE Global Commun. Conf. (GLOBECOM)*, 2019, pp. 1–6.
- [51] C. Yue, M. Shirvanimoghaddam, B. Vucetic, and Y. Li, "A revisit to ordered statistics decoding: Distance distribution and decoding rules," *IEEE Trans. Inf. Theory*, vol. 67, no. 7, pp. 4288–4337, 2021.
- [52] L. Yang, W. Chen, and L. Chen, "Reduced complexity ordered statistics decoding of linear block codes," in *2022 IEEE/CIC International Conference on Communications in China (ICCC Workshops)*, 2022, pp. 371–376.
- [53] A. d. iOlius and J. E. Martinez, "The closed-branch decoder for quantum ldpc codes," *arXiv preprint arXiv:2402.01532*, 2024.
- [54] A. Gong, S. Cammerer, and J. M. Renes, "Toward low-latency iterative decoding of qlpdc codes under circuit-level noise," *arXiv preprint arXiv:2403.18901*, 2024.
- [55] S. Bravyi, A. W. Cross, J. M. Gambetta, D. Maslov, P. Rall, and T. J. Yoder, "High-threshold and low-overhead fault-tolerant quantum memory," *Nature*, vol. 627, no. 8005, pp. 778–782, 2024.
- [56] S. Wolanski and B. Barber, "Ambiguity clustering: an accurate and efficient decoder for QLDPC codes," *arXiv preprint arXiv:2406.14527*, 2024.
- [57] T. Hillmann, L. Berent, A. O. Quintavalle, J. Eisert, R. Wille, and J. Roffe, "Localized statistics decoding: A parallel decoding algorithm for quantum low-density parity-check codes," *arXiv preprint arXiv:2406.18655*, 2024.
- [58] A. A. Kovalev, I. Dumer, and L. P. Pryadko, "Design of additive quantum codes via the code-word-stabilized framework," *Phys. Rev. A*, vol. 84, no. 6, p. 062319, 2011.
- [59] J. Old, M. Rispler, and M. Müller, "Lift-connected surface codes," *Quantum Science and Technology*, vol. 9, no. 4, p. 045012, jul 2024. [Online]. Available: <https://dx.doi.org/10.1088/2058-9565/ad5eb6>
- [60] M.-H. Hsieh and F. Le Gall, "NP-hardness of decoding quantum error-correction codes," *Phys. Rev. A*, vol. 83, p. 052331, 2011.
- [61] K.-Y. Kuo and C.-C. Lu, "On the hardnesses of several quantum decoding problems," *Quant. Inf. Process.*, vol. 19, no. 4, pp. 1–17, 2020.
- [62] P. Iyer and D. Poulin, "Hardness of decoding quantum stabilizer codes," *IEEE Trans. Inf. Theory*, vol. 61, no. 9, pp. 5209–5223, 2015.
- [63] M. Hagiwara, M. P. C. Fossorier, and H. Imai, "Fixed initialization decoding of LDPC codes over a binary symmetric channel," *IEEE Trans. Inf. Theory*, vol. 58, no. 4, pp. 2321–2329, 2012.
- [64] K.-Y. Kuo and C.-Y. Lai, "Comparison of 2D topological codes and their decoding performances," in *Proc. IEEE Int. Symp. Inf. Theory (ISIT)*, 2022, pp. 186–191.
- [65] J. Chen, Z. Yi, Z. Liang, and X. Wang, "Improved belief propagation decoding algorithms for surface codes," *arXiv preprint arXiv:2407.11523*, 2024.
- [66] C. Wang, J. Harrington, and J. Preskill, "Confinement-Higgs transition in a disordered gauge theory and the accuracy threshold for quantum memory," *Annals of Physics*, vol. 303, no. 1, pp. 31–58, 2003.
- [67] C. T. Chubb, "General tensor network decoding of 2d pauli codes," 2021. [Online]. Available: <https://arxiv.org/abs/2101.04125>
- [68] J. Edmonds, "Paths, trees, and flowers," *Canadian Journal of Mathematics*, vol. 17, pp. 449–467, 1965.
- [69] D. S. Wang, A. G. Fowler, A. M. Stephens, and L. C. L. Hollenberg, "Threshold error rates for the toric and planar codes," *Quant. Inf. Comput.*, vol. 10, no. 5, pp. 456–469, 2010.
- [70] S. Gounai and T. Ohtsuki, "Decoding algorithms based on oscillation for low-density parity check codes," *IEICE Trans. Fundam. Electron. Commun. Comput. Sci.*, vol. 88, no. 8, pp. 2216–2226, 2005.
- [71] S. Gounai, T. Ohtsuki, and T. Kaneko, "Modified belief propagation decoding algorithm for low-density parity check code based on oscillation," in *IEEE Veh. Technol. Conf. (VTC)*, vol. 3, 2006, pp. 1467–1471.
- [72] M. Jiang, C. Zhao, E. Xu, and L. Zhang, "Reliability-based iterative decoding of ldpc codes using likelihood accumulation," *IEEE Commun. Lett.*, vol. 11, no. 8, pp. 677–679, 2007.
- [73] J. Rosseel, V. Mannoni, V. Savin, and I. Fijalkow, "Sets of complementary LLRs to improve OSD post-processing of BP decoding," in *2023 12th International Symposium on Topics in Coding (ISTC)*. IEEE, 2023, pp. 1–5.
- [74] A. O. Quintavalle, M. Vasmer, J. Roffe, and E. T. Campbell, "Single-shot error correction of three-dimensional homological product codes," *PRX Quantum*, vol. 2, p. 020340, 2021.
- [75] O. Higgott and N. P. Breuckmann, "Improved single-shot decoding of higher dimensional hypergraph product codes," 2022. [Online]. Available: <https://arxiv.org/abs/2206.03122>
- [76] A. Ashikhmin, C.-Y. Lai, and T. A. Brun, "Quantum data-syndrome codes," *IEEE J. Sel. Area. Comm.*, vol. 38, no. 3, pp. 449 – 462, 2020.
- [77] K.-Y. Kuo, I.-C. Chern, and C.-Y. Lai, "Decoding of quantum data-syndrome codes via belief propagation," in *Proc. IEEE Int. Symp. Inf. Theory (ISIT)*, 2021, pp. 1552–1557.
- [78] K.-Y. Kuo and C.-Y. Lai, "Correcting phenomenological quantum noise via belief propagation," *arXiv preprint*, 2023. [Online]. Available: <https://arxiv.org/abs/2310.12682>
- [79] L. P. Pryadko, "On maximum-likelihood decoding with circuit-level errors," *Quantum*, vol. 4, p. 304, 2020.
- [80] J. Du Crest, M. Mhalla, and V. Savin, "Stabilizer inactivation for message-passing decoding of quantum LDPC codes," in *2022 IEEE Information Theory Workshop (ITW)*. IEEE, 2022, pp. 488–493.
- [81] J. du Crest, F. Garcia-Herrero, M. Mhalla, V. Savin, and J. Valls, "Check-agnosia based post-processor for message-passing decoding of quantum LDPC codes," *Quantum*, vol. 8, p. 1334, 2024.
- [82] T. R. Scruby, T. Hillmann, and J. Roffe, "High-threshold, low-overhead and single-shot decodable fault-tolerant quantum memory," *arXiv preprint arXiv:2406.14445*, 2024.
- [83] A. d. iOlius, I. E. Martinez, J. Roffe, and J. E. Martinez, "An almost-linear time decoding algorithm for quantum LDPC codes under circuit-level noise," *arXiv preprint arXiv:2409.01440*, 2024.
- [84] C. Gidney, "Stim: a fast stabilizer circuit simulator," *Quantum*, vol. 5, p. 497, 2021.